Transport Processes and Separation Process Principles

(INCLUDES UNIT OPERATIONS)

FOURTH EDITION

CHRISTIE JOHN GEANKOPLIS

Table of Contents

Chapter 13. Membrane Separation Processes

Chapter 13. Membrane Separation Processes

INTRODUCTION AND TYPES OF MEMBRANE SEPARATION PROCESSES

Introduction

Separations by the use of membranes are becoming increasingly important in the process industries. In this relatively new separation process, the membrane acts as a semipermeable barrier and separation occurs by the membrane controlling the rate of movement of various molecules between two liquid phases, two gas phases, or a liquid and a gas phase. The two fluid phases are usually miscible and the membrane barrier prevents actual, ordinary hydro-dynamic flow. A classification of the main types of membrane separation follows.

Classification of Membrane Processes

Gas diffusion in porous solid

In this type a gas phase is present on both sides of the membrane, which is a microporous solid. The rates of molecular diffusion of the various gas molecules depend on the pore sizes and the molecular weights. This type of diffusion in the molecular, transition, and Knudsen regions was discussed in detail in Section 7.6.

Liquid permeation or dialysis

In this case, the small solutes in one liquid phase diffuse readily because of concentration differences through a porous membrane to the second liquid (or vapor) phase. Passage of large molecules through the membrane is more difficult. This membrane process has been applied in chemical processing separations such as separation of H_2SO_4 from nickel and copper sulfates in aqueous solutions, food processing, and artificial kidneys, and will be covered in detail in Section 13.2. In electrodialysis, separation of ions occurs by imposing an emf difference across the membrane.

Gas permeation in a membrane

The membrane in this process is usually a polymer such as rubber, polyamide, and so on, and is not a porous solid. The solute gas first dissolves in the membrane and then diffuses in the solid to the other gas phase. This was discussed in detail in Section 6.5 for solutes following Fick's law and will be considered again, for the case where resistances are present, in Section 13.3A. In Sections 13.3 to 13.8, different process flow patterns are considered. Examples of membrane separations are helium being separated from natural gas and nitrogen from air. Separation of a gas mixture occurs because each type of molecule diffuses at a different rate through the membrane.

Reverse osmosis

A membrane, which impedes the passage of a low-molecular-weight solute, is placed between a solute-solvent solution and a pure solvent. The solvent diffuses into the solution by osmosis. In reverse osmosis, a reverse pressure difference is imposed which causes the flow of solvent to reverse, as in the desalination of seawater. This process is also used to separate other low-molecular-weight solutes, such as salts, sugars, and simple acids from a solvent (usually water). This process will be covered in detail in Sections 13.9 and 13.10.

Ultrafiltration membrane process

In this process, pressure is used to obtain a separation of molecules by means of a semipermeable polymeric membrane (M2). The membrane discriminates on the basis of molecular size, shape, or chemical structure and separates relatively high-molecular-weight solutes such as proteins, polymers, colloidal materials such as minerals, and so on. The osmotic pressure is usually negligible because of the high molecular weights. This will be covered in Section 13.11.

Microfiltration membrane process

In microfiltration, pressure-driven flow through the membrane is used to separate micron-size particles from fluids. The particles are usually larger than those in ultrafiltration. Examples are separation of bacteria, paint pigment, yeast cells, and so on from solutions. This process will be covered in Section 13.12.

Gel permeation chromotography

The porous gel retards diffusion of the high-molecular-weight solutes. The driving force is concentration. This process is quite useful in analyzing complex chemical solutions and in the purification of very specialized and/or valuable components.

LIQUID PERMEATION MEMBRANE PROCESSES OR DIALYSIS

Series Resistances in Membrane Processes

In membrane processes with liquids, the solute molecules must first be transported or diffuse through the liquid film of the first liquid phase on one side of the solid membrane, then through the membrane itself, and finally through the film of the second liquid phase. This is shown in Fig. 13.2-1a, where c_1 is the bulk liquid-phase concentration of the diffusing solute A in kg mol A/m^3, c_{1i} is the concentration of A in the fluid just adjacent to the solid, and c_{1iS} is the concentration of A in the solid at the surface and is in equilibrium with C_{1i}. The mass-transfer coefficients are k_{c1} and k_{c2} in m/s. The equilibrium distribution coefficient K' is defined as

Equation 13.2-1.

$$K' = \frac{c_S}{c_L} = \frac{c_{1iS}}{c_{1i}} = \frac{c_{2iS}}{c_{2i}}$$

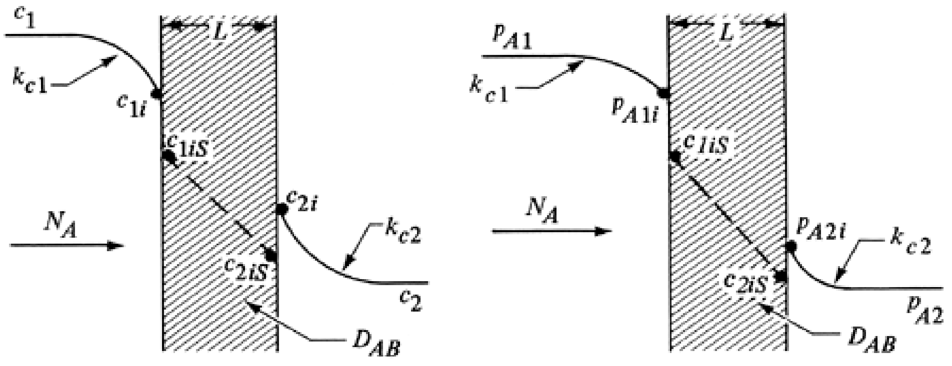

(a) (b)

Figure 13.2-1. Concentration profiles for membrane processes: (a) two liquid films and a solid, (b) two gas films and a solid.

Note that K' is the inverse of K defined in Eq. (7.1-16).

The flux equations through each phase are all equal to each other at steady state and are as follows:

Equation 13.2-2.

$$N_A = k_{c1}(c_1 - c_{1i}) = \frac{D_{AB}}{L}(c_{1iS} - c_{2iS}) = k_{c2}(c_{2i} - c_2)$$

Substituting $c_{1iS} = K'c_{1i}$ and $c_{2iS} = K'c_{2i}$ into Eq. (13.2-2),

Equation 13.2-3.

$$N_A = k_{c1}(c_1 - c_{1i}) = \frac{D_{AB}K'}{L}(c_{1i} - c_{2i}) = p_M(c_{1i} - c_{2i}) = k_{c2}(c_{2i} - c_2)$$

Equation 13.2-4.

$$p_M = \frac{D_{AB}K'}{L}$$

where p_M is the permeance in the solid in m/s, L is the thickness in m, and D_{AB} is the diffusivity of A in the solid in m^2/s. Note that the permeance p_M in Eq. (13.2-4) is different from the permeability P_M defined in Eq. (6.5-9). Also, the value of p_M is inversely proportional to the thickness L. Instead of determining D_{AB} and K' in two separate experiments, it is more convenient to determine p_M in one separate diffusion experiment. Solving each of the parts of Eq. (13.2-3) for the concentration difference,

Equation 13.2-5.

$$c_1 - c_{1i} = \frac{N_A}{k_{c1}} \qquad c_{1i} - c_{2i} = \frac{N_A}{p_M} \qquad c_{2i} - c_2 = \frac{N_A}{k_{c2}}$$

Adding the equations, the internal concentrations c_{1i} and c_{2i} drop out, and the final equation is

Equation 13.2-6.

$$N_A = \frac{c_1 - c_2}{1/k_{c1} + 1/p_M + 1/k_{c2}}$$

In some cases, the resistances in the two liquid films are quite small compared to the membrane resistance, which controls the permeation rate.

EXAMPLE 13.2-1. Membrane Diffusion and Liquid Film Resistances

A liquid containing dilute solute A at a concentration $c_1 = 3 \times 10^{-2}$ kg mol/m^3 is flowing rapidly past a membrane of thickness $L = 3.0 \times 10^{-5}$ m. The distribution coefficient $K' = 1.5$ and $D_{AB} = 7.0 \times 10^{-11}$ m^2/s in the membrane. The solute diffuses through the membrane, and its concentration on the other side is $c_2 = 0.50 \times 10^{-2}$ kg mol/m^3. The mass-transfer coefficient k_{c1} is large and can be considered as infinite, and $k_{c2} = 2.02 \times 10^{-5}$ m/s.

a. Derive the equation to calculate the steady-state flux N_A and make a sketch.

b. Calculate the flux and the concentrations at the membrane interfaces.

Solution: For part (a), the sketch is shown in Fig. 13.2-2. Note that the concentration profile on the left side is flat ($k_{c1} = \infty$) and $c_1 = c_{1i}$. The derivation is the same as for Eq. (13.2-6), but $1/k_{c1} = 0$ to give

Equation 13.2-7.

$$N_A = \frac{c_1 - c_2}{1/p_M + 1/k_{c2}}$$

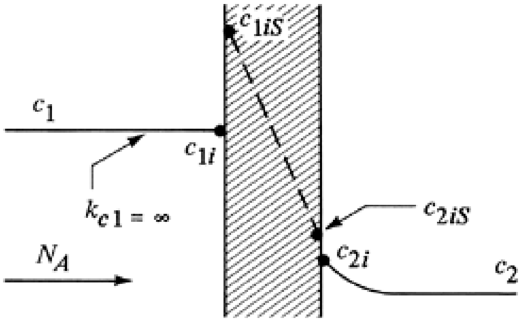

Figure 13.2-2. Concentrations for Example 13.2-1.

For part (b), to calculate the flux using Eqs. (13.2-4) and (13.2-7),

$$p_M = \frac{D_{AB}K'}{L} = \frac{7.0 \times 10^{-11}(1.5)}{3.0 \times 10^{-5}} = 3.5 \times 10^{-6} \text{ m/s}$$

$$N_A = \frac{c_1 - c_2}{1/p_M + 1/k_{c2}} = \frac{3.0 \times 10^{-2} - 0.5 \times 10^{-2}}{1/3.5 \times 10^{-6} + 1/2.02 \times 10^{-5}}$$

$$= 7.458 \times 10^{-8} \text{ kg mol/s} \cdot \text{m}^2$$

To calculate c_{2i},

$$N_A = 7.458 \times 10^{-8} = k_{c2}(c_{2i} - c_2) = 2.02 \times 10^{-5}(c_{2i} - 0.5 \times 10^{-2})$$

Solving, $c_{2i} = 0.869 \times 10^{-2}$ kg mol/m^3. Also, using Eq. (13.2-1),

$$K' = 1.5 = \frac{c_{2iS}}{c_{2i}} = \frac{c_{2iS}}{0.869 \times 10^{-2}}$$

Solving, $c_{2is} = 1.304 \times 10^{-2}$ kg mol/m^3.

Dialysis Processes

Dialysis uses a semipermeable membrane to separate species by virtue of their different diffusion rates in the membrane. The feed solution or dialyzate, which contains the solutes to be separated, flows on one side of the membrane and the solvent or diffusate stream on the other side. Some solvent may also diffuse across the membrane in the opposite direction, which reduces performance by diluting the dialyzate.

In practice dialysis is used to separate species which differ appreciably in size and thus have a reasonably large difference in diffusion rates. Solute fluxes depend on the concentration gradient in the membrane. Hence, dialysis is characterized by low flux rates in comparison to other membrane processes, such as reverse osmosis and ultrafiltration, which depend on applied pressure.

In general, dialysis is used with aqueous solutions on both sides of the membrane. The film resistances can be appreciable compared to the membrane resistance. Applications include recovery of sodium hydroxide in cellulose processing, recovery of acids from metallurgical liquors, removal of products from a culture solution in fermentation, desalting of cheese whey solids, and reduction of alcohol content of beer. Many small-scale applications occur in the pharmaceutical industry.

Types of Equipment for Dialysis

Various geometrical configurations are used in liquid membrane processes. A common one is similar to a filter press, where the membrane is a flat plate. Vertical solid membranes are placed in between alternating liquor and solvent feed frames, with the liquor to be dialyzed being fed to the bottom and the solvent to the top of these frames. The dialyzate and the diffusate are removed through channels located at the top and bottom of the frames, respectively. The most important type consists of many small tubes or very fine hollow fibers arranged in a bundle, like a heat exchanger. This type of unit has a very high ratio of membrane area to volume of the unit.

Hemodialysis in Artificial Kidney

An important example of the liquid permeation process is dialysis with an artificial kidney in the biomedical field. In this application for purifying human blood, the principal solutes removed are the small solutes urea, uric acid, creatinine, phosphates, and excess amounts of chloride. A typical membrane used is cellophane about 0.025 mm thick, which allows small solutes to diffuse but retains the large proteins in the blood. During the hemodialysis, blood is passed on one side of the membrane while an aqueous dialyzing fluid flows on the other side. Solutes such as urea, uric acid, NaCl, and so on, which have elevated concentrations in the blood, diffuse across the membrane to the dialyzing aqueous solution, which contains certain concentrations of solutes such as potassium salts, and so on, to ensure that concentrations in the blood do not drop below certain levels. In one configuration the membranes are stacked in the form of a multilayered sandwich, with blood flowing past one side of the membrane and dialyzing fluid past the other side. The hollow fiber type is used quite often.

EXAMPLE 13.2-2. Dialysis to Remove Urea from Blood

Calculate the flux and the rate of removal of urea at steady state in g/h from blood in a cuprophane (cellophane) membrane dialyzer at 37°C. The membrane is 0.025 mm thick and has an area of 2.0 m^2. The mass-transfer coefficient on the blood side is estimated as $k_{c1} = 1.25 \times 10^{-5}$ m/s and that on the aqueous side is 3.33×10^{-5} m/s. The permeance of the membrane is 8.73×10^{-6} m/s (B2). The concentration of urea in the blood is 0.02 g urea/100 mL and that in the dialyzing fluid will be assumed as 0.

Solution: The concentration $c_1 = 0.02/100 = 2.0 \times 10^{-4}$ g/mL = 200 g/m^3 and $c_2 = 0$. Substituting into Eq. (13.2-6),

$$N_A = \frac{c_1 - c_2}{1/k_{c1} + 1/p_M + 1/k_{c2}}$$

$$= \frac{200 - 0}{1/1.25 \times 10^{-5} + 1/8.73 \times 10^{-6} + 1/3.33 \times 10^{-5}}$$

$$= 8.91 \times 10^{-4}\ \mathrm{g/s \cdot m^2}$$

For a time of 1 h and an area of 2.0 m^2,

$$\text{rate of removal} = 8.91 \times 10^{-4}(3600)(2.0) = 6.42\ \text{g urea/h}$$

GAS PERMEATION MEMBRANE PROCESSES

Series Resistances in Membrane Processes

In membrane processes with two gas phases and a solid membrane, similar equations can be written for the case illustrated in Fig. 13.2-1b. The equilibrium relation between the solid and gas phases is given by

Equation 13.3-1.

$$H = \frac{S}{22.414} = \frac{c_S}{p_A} = \frac{c_{1iS}}{p_{A1i}} = \frac{c_{2iS}}{p_{A2i}}$$

where S is the solubility of A in m^3 (STP)/atm · m^3 solid, as shown in Eq. (6.5-5), and H is the equilibrium relation in kg mol/m^3 · atm. This is similar to Henry's law. The flux equations in each phase are as follows:

Equation 13.3-2.

$$N_A = \frac{k_{c1}}{RT}(p_{A1} - p_{A1i}) = \frac{D_{AB}}{L}(c_{1iS} - c_{2iS})$$

Equation 13.3-3.

$$= \frac{D_{AB}S}{L(22.414)}(p_{A1i} - p_{A2i})$$

Equation 13.3-4.

$$= \frac{k_{c2}}{RT}(p_{A2i} - p_{A2})$$

The permeability P_M given previously is

Equation 6.5-9.

$$P_M = D_{AB}S\frac{\mathrm{m^3\,(STP) \cdot m}}{\mathrm{s \cdot m^2 C.S. \cdot atm}}$$

The permeability P_M is given in kg mol units by dividing Eq. (6.5-9) by 22.414 m^3/kg mol:

Equation 13.3-5.

$$1.00 \frac{\text{kg mol} \cdot \text{m}}{\text{s} \cdot \text{m}^2\text{C.S.} \cdot \text{atm}} = \frac{1}{22.414} \frac{\text{m}^3\,(\text{STP}) \cdot \text{m}}{\text{s} \cdot \text{m}^2\text{C.S.} \cdot \text{atm}}$$

Then the flux N_A through the membrane given by Eq. (13.3-3) becomes

Equation 13.3-6.

$$N_A = \frac{P_M}{L}(p_{A1i} - p_{A2i})$$

Eliminating the interfacial concentrations as before,

Equation 13.3-7.

$$N_A = \frac{(p_{A1} - p_{A2})}{1/(k_{c1}/RT) + 1/(P_M/L) + 1/(k_{c2}/RT)}$$

In the case where pure A (p_{A1}) is on the left side of the membrane, there is no diffusional resistance in the gas phase, and k_{c1} can be considered to be infinite. Note that $k_{G1} = k_{c1}/RT$.

An example of gas permeation in a membrane is the use of a polymeric membrane as an oxygenator for a heart-lung machine to oxygenate blood. In this biomedical application, pure O_2 gas is on one side of a thin membrane and blood is on the other side. Oxygen diffuses through the membrane into the blood and CO_2 diffuses in a reverse direction into the gas stream.

Types of Membranes and Permeabilities for Separation of Gases

Types of dense-phase symmetric membranes

Early membranes were limited in their use because of low selectivities in separating two gases and quite low permeation fluxes. This low-flux problem was due to the fact that the membranes had to be relatively thick (1 mil or 1/1000 of an inch or greater) in order to avoid tiny holes, which reduced the separation by allowing viscous or Knudsen flow of the feed. Development of silicone polymers (1 mil thickness) increased the permeability by factors of 10–20 or so. These are called dense-phase symmetric membranes.

Types of asymmetric membranes

Newer asymmetric membranes include a very thin but dense skin on one side of the membrane supported by a porous substructure (R1). The dense skin has a thickness of about 1000 Å and the porous support thickness is about 25–100 μm. The flux increase of these membranes is thousands of time higher than the 1-mil-thick original membranes. Some typical materials currently used for asymmetric membranes are a composite of polysulfone coated with silicone rubber, cellulose acetate and modified cellulose acetates, aromatic polyamides or aromatic polyimides, and silicone-polycarbonate copolymer on a porous support.

Permeability of membranes

The permeability P_M in Eqs. (6.5-9) and (13.3-6) is defined as $D_{AB}S$ in m^3 (STP)/s · m^2C.S. · atm/m. Since mixtures of gases are often present, P'_A for gas A and P'_B for gas B will be used instead of P_M. The different sets of units used and their conversion factors are given in Table 13.3-1. Sometimes units are given in terms of Barrers, as also defined in Table 13.3-1.

Table 13.3-1. Conversion Factors for Permeability P'_A and Permeance P'_A/t

Permeability, P'_A	*Permeance,* P'_A/t
$\frac{1.00\ \text{cm}^3\ (\text{STP})\cdot\text{cm}}{\text{s}\cdot\text{cm}^2\cdot\text{cm Hg}} = 7.501\times10^{-8}\frac{\text{m}^3\ (\text{STP})\cdot\text{m}}{\text{s}\cdot\text{m}^2\cdot\text{Pa}}$	$\frac{1.00\ \text{cm}^3\ (\text{STP})}{\text{s}\cdot\text{cm}^2\cdot\text{cm Hg}} = 7.501\times10^{-6}\frac{\text{m}^3\ (\text{STP})}{\text{s}\cdot\text{m}^2\cdot\text{Pa}}$
$1.00\ \text{Barrer} = 10^{-10}\frac{\text{cm}^3\ (\text{STP})\cdot\text{cm}}{\text{s}\cdot\text{cm}^2\cdot\text{cm Hg}}$	$1.00\ \text{Barrer/cm} = 10^{-10}\frac{\text{cm}^3\ (\text{STP})}{\text{s}\cdot\text{cm}^2\cdot\text{cm Hg}}$
$\frac{1.00\ \text{cm}^3\ (\text{STP})\cdot\text{cm}}{\text{s}\cdot\text{cm}^2\cdot\text{cm Hg}} = 480.9\frac{\text{ft}^3\ (\text{STP})\cdot\text{ft}}{\text{day}\cdot\text{ft}^2\cdot\text{psi}}$	$\frac{1.00\ \text{cm}^3\ (\text{STP})}{\text{s}\cdot\text{cm}^2\cdot\text{cm Hg}} = 1.4659\times10^{4}\frac{\text{ft}^3\ (\text{STP})}{\text{day}\cdot\text{ft}^2\cdot\text{psi}}$
$\frac{1.00\ \text{cm}^3\ (\text{STP})\cdot\text{cm}}{\text{s}\cdot\text{cm}^2\cdot\text{cm Hg}} = 20.04\frac{\text{ft}^3\ (\text{STP})\cdot\text{ft}}{\text{hr}\cdot\text{ft}^2\cdot\text{psi}}$	$\frac{1.00\ \text{cm}^3\ (\text{STP})}{\text{s}\cdot\text{cm}^2\cdot\text{cm Hg}} = 610.8\frac{\text{ft}^3\ (\text{STP})}{\text{hr}\cdot\text{ft}^2\cdot\text{psi}}$

The accurate prediction of permeabilities of gases in membranes is generally not possible, and experimental values are needed. Experimental data for common gases in some typical dense-phase membranes are given in Table 13.3-2. Note that there are wide differences among the permeabilities of various gases in a given membrane. Silicone rubber exhibits very high permeabilities for the gases in the table.

Table 13.3-2. Permeabilities of Various Gases in Dense-Phase Symmetric Membranes

		Permeability, $P'_A,\ \frac{cm^3(STP)\cdot cm}{s\cdot cm^2\cdot cm\ Hg}\times10^{10}$						
Material	***Temp. (°C)***	***He***	H_2	CH_4	CO_2	O_2	N_2	***Ref.***
Silicone rubber	25	300	550	800	2700	500	250	(S2)
Natural rubber	25	31	49	30	131	24	8.1	(S2)
Polycarbonate (Lexane)	25–30	15	12		5.6,10	1.4		(S2)
Nylon 66	25	1.0			0.17	0.034	0.008	(S2)
Polyester (Permasep)	—		1.65	0.035	0.31		0.031	(H1)
Silicone-polycarbonate copolymer (57% silicone)	25		210		970	160	70	(W2)
Teflon FEP	30	62		1.4			2.5	(S1)
Ethyl cellulose	30	35.7	49.2	7.47	47.5	11.2	3.29	(W3)
Polystyrene	30	40.8	56.0	2.72	23.3	7.47	2.55	(W3)

For the effect of temperature T in K, ln P'_A is approximately a linear function of $1/T$ and increases with T. However, operation at high temperatures can often degrade the membranes. When a mixture of gases is present, reductions of permeability of an individual component of up to 10% or so can often occur. In a few cases, much larger reductions have been observed (R1). Hence, when using a mixture of gases, experimental data should be obtained to determine if there is any interaction between the gases. The presence of water vapor can have similar effects on the permeabilities and can also possibly damage the membranes.

Permeance of membranes

In many cases, especially in asymmetric membranes, the thickness t is not measured and only experimental values of permeance P'_A/t are given. Conversion factors are also given in Table 13.3-1.

Types of Equipment for Gas Permeation Membrane Processes

Flat membranes

Flat membranes are mainly used in experiments to characterize the permeability of the membrane. The modules are easy to fabricate and use and the areas of the membranes are well defined. In some cases modules are stacked together like a multilayer sandwich or plate-and-frame filter press. The major drawback of this type is the very small membrane area per unit separator volume. Small commercial flat membranes are used for producing oxygen-enriched air for individual medical applications.

Spiral-wound membranes

This configuration retains the simplicity of fabricating flat membranes while increasing markedly the membrane area per unit separator volume up to 100 ft^2/ft^3 (328 m^2/m^3) and decreasing pressure drops (R1). The assembly consists of a sandwich of four sheets wrapped around a central core of a perforated collecting tube. The four sheets consist of a top sheet of an open separator grid for the feed channel, a membrane, a porous felt backing for the permeate channel, and another membrane, as shown in Fig. 13.3-1. The spiral-wound element is 100 to 200 mm in diameter and is about 1 to 1.5 m long in the axial direction. The flat sheets before rolling are about 1-1.5 m by about 2-2.5 m. The space between the membranes (open grid for feed) is about 1 mm and the thickness of the porous backing (for permeate) is about 0.2 mm.

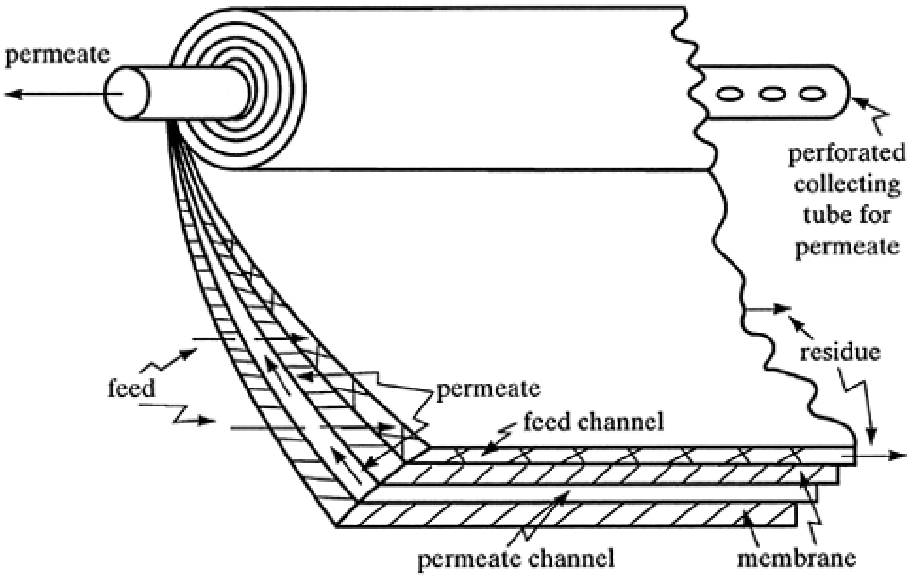

*Figure 13.3-1. Spiral-wound elements and assembly. [From R. I. Berry, Chem. Eng., **88** (July 13), 63 (1981). With permission.]*

The whole spiral-wound element is located inside a metal shell. The feed gas enters at the left end of the shell, enters the feed channel, and flows through this channel in the axial direction of the spiral to the right end of the assembly (Fig. 13.3-1). Then the exit residue gas leaves the shell at this point. The feed stream, which is in the feed channel, permeates perpendicularly through the membrane.

This permeate then flows through the permeate channel in a direction perpendicular to the feed stream toward the perforated collecting tube, where it leaves the apparatus at one end. This is illustrated in Fig. 13.3-2, where the local gas flow paths are shown for a small element of the assembly.

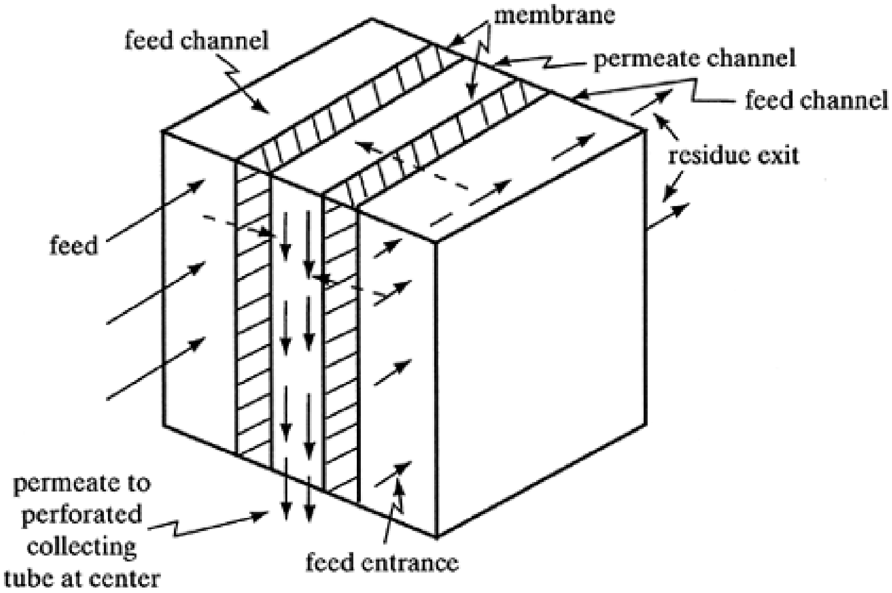

Figure 13.3-2. Local gas flow paths for spiral-wound separator.

Hollow-fiber membranes

The membranes are in the shape of very-small-diameter hollow fibers. The inside diameter of the fibers is in the range of 100–500 μm and the outside 200–1000 μm, with the length up to 3-5 m. The module resembles a shell-and-tube heat exchanger. Thousands of fine tubes are bound together at each end into a tube sheet that is surrounded by a metal shell having a diameter of 0.1-0.2 m, so that the membrane area per unit volume is up to 10 000 m^2/m^3, as in Fig. 13.3-3. A typical large industrial permeator has fibers of 200 μm ID and 400 μm OD in a shell 6 in. in diameter and 10 ft long (P7).

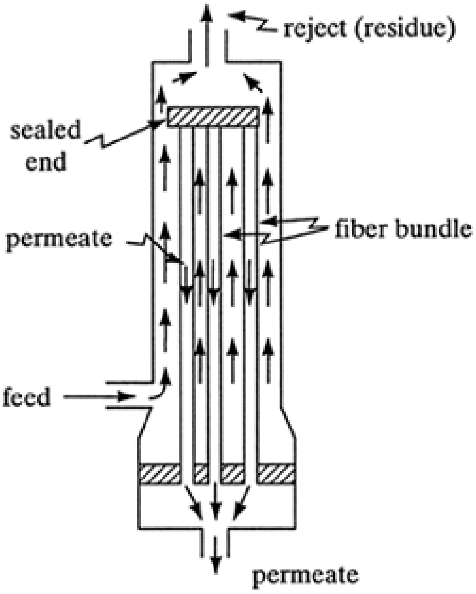

Figure 13.3-3. Hollow-fiber separator assembly.

Typically, the high-pressure feed enters the shell side at one end and leaves at the other end. The hollow fibers are closed at one end of the tube bundles. The permeate gas inside the fibers flows countercurrent to the shell-side flow and is collected in a chamber where the open ends of the fibers terminate. Then the permeate exits the device.

In some lower-pressure operations, such as for separation of air to produce nitrogen, the feed enters inside the tubes (P7).

Introduction to Types of Flow in Gas Permeation

Types of flow and diffusion gradients

In a membrane process, high-pressure feed gas is supplied to one side of the membrane and permeates normal to the membrane. The permeate leaves in a direction normal to the membrane, accumulating on the low-pressure side. Because of the very high diffusion coefficient in gases, concentration gradients in the gas phase in the direction normal to the surface of the membrane are quite small. Hence, gas film resistances compared to the membrane resistance can be neglected. This means that the concentration in the gas phase in a direction perpendicular to the membrane is essentially uniform, whether the gas stream is flowing parallel to the surface or is not flowing.

If the gas stream is flowing parallel to the membrane in essentially plug flow, a concentration gradient occurs in this direction. Hence, several cases can occur in the operation of a membrane module. The permeate side of the membrane can be operated so that the phase is completely mixed (uniform concentration) or so that the phase is in plug flow. The high-pressure feed side can also be completely mixed or in plug flow. Countercurrent or cocurrent flow can be used when both sides are in plug flow. Hence, separate theoretical models must be derived for these different types of operation, as given in Sections 13.4–13.8.

Assumptions used and ideal flow patterns

In deriving theoretical models for gas separation by membranes, isothermal conditions and negligible pressure drop in the feed stream and permeate stream are generally assumed. It is also assumed that the effects of total pressure and/or composition of the gas are negligible and that the permeability of each component is constant (i.e., no interactions between different components).

Since there are a number of idealized flow patterns, the important types are summarized in Fig. 13.3-4. In Fig. 13.3-4a, complete mixing is assumed for the feed chamber and the permeate chamber. Similar to a continuous-stirred tank, the reject or residue and the product or permeate compositions are equal to their respective uniform compositions in the chambers.

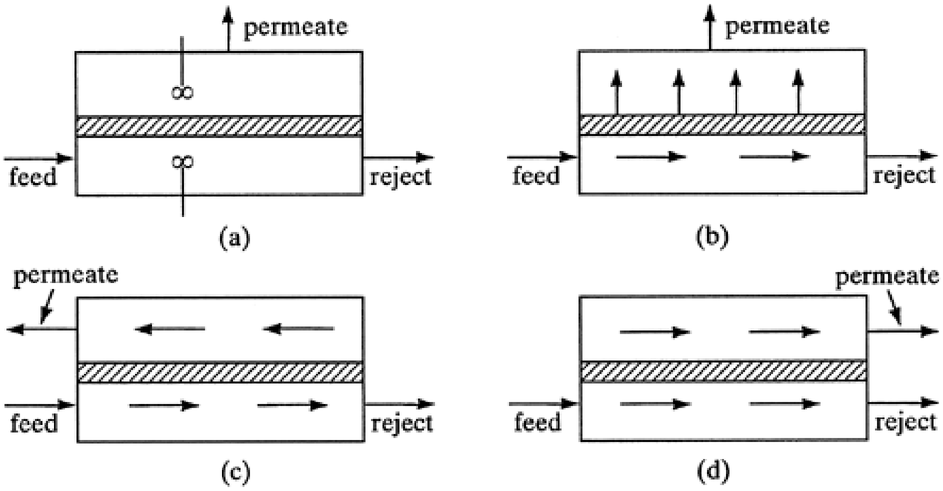

Figure 13.3-4. Ideal flow patterns in a membrane separator for gases: (a) complete mixing, (b) cross-flow, (c) countercurrentflow, (d) cocurrent flow.

An ideal cross-flow pattern is given in Fig. 13.3-4b, where the feed stream is in plug flow and the permeate flows in a normal direction away from the membrane without mixing. Since the feed composition varies along its flow path, the local permeate concentration also varies along the membrane path.

In Fig. 13.3-4c, both the feed stream and permeate stream are in plug flow countercurrent to each other. The composition of each stream varies along its flow path. Cocurrent flow of the feed and permeate streams is shown in Fig. 13.3-4d.

COMPLETE-MIXING MODEL FOR GAS SEPARATION BY MEMBRANES

Basic Equations Used

In Fig. 13.4-1, a detailed process flow diagram is shown for complete mixing. When a separator element is operated at a low recovery (i.e., where the permeate flow rate is a small fraction of the entering feed rate), there is a minimal change in composition. Then the results derived using the complete-mixing model provide reasonable estimates of permeate purity. This case was derived by Weller and Steiner (W4).

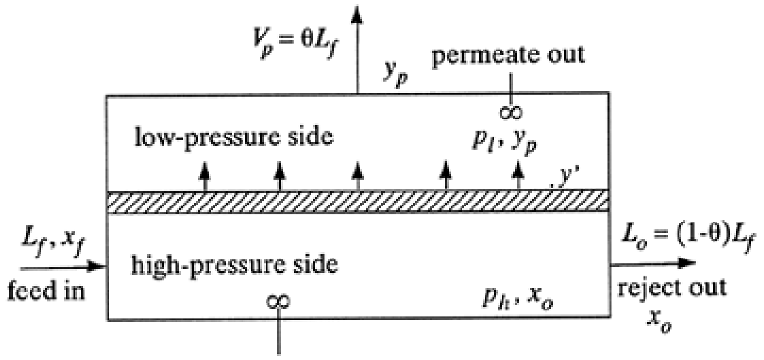

Figure 13.4-1. Process flow for complete mixing case.

Using nomenclature similar to that for distillation (P7), using the feed and nonpermeate flow rate as *L* and composition *x* mole fraction and the permeate flow rate as *V* and composition *y*.

The overall material balance (Fig. 13.4-1) is as follows:

Equation 13.4-1.

$$L_f = L_o + V_p$$

where L_f is total feed flow rate in cm^3 (STP)/s; L_o is outlet reject flow rate, cm^3 (STP)/s; and V_p is outlet permeate flow rate, cm^3 (STP)/s. The cut or fraction of feed permeated, θ, is given as

Equation 13.4-2.

$$\theta = \frac{V_p}{L_f}$$

The rate of diffusion or permeation of species *A* (in a binary of *A* and *B*) is given below by an equation similar to Eq. (13.3-6) but using cm^3 (STP)/s as rate of permeation rather than flux in kg mol/s · cm^2:

Equation 13.4-3.

$$\frac{V_A}{A_m} = \frac{V_p y_p}{A_m} = \left(\frac{P'_A}{t}\right)(p_h x_o - p_l y_p)$$

where P'_A is permeability of *A* in the membrane, cm^3 (STP) · cm/(s · cm^2 · cm Hg); V_A is flow rate of *A* in permeate, cm^3 (STP)/s; A_m is membrane area, cm^2; *t* is membrane thickness, cm; p_h is total pressure in the high-pressure (feed) side, cm Hg; p_l is total pressure in the low-pressure or permeate side, cm Hg: x_o is mole fraction of *A* in reject side; x_f is mole fraction of *A* in feed; and y_p is mole fraction of *A* in permeate. Note that $p_h x_o$ is the partial pressure of *A* in the reject gas phase and $p_l y_p$ is the partial pressure in the permeate side. A similar equation can be written for component *B*.

Equation 13.4-4.

$$\frac{V_B}{A_m} = \frac{V_p(1 - y_p)}{A_m} = \left(\frac{P'_B}{t}\right)[p_h(1 - x_o) - p_l(1 - y_p)]$$

Where P'_B is permeability of *B,* cm^3 (STP) · cm/(s · cm^2 · cm Hg). The ideal separation factor α^* is

Equation 13.4-5.

$$\alpha^* = P'_A/P'_B$$

Dividing Eq. (13.4-3) by (13.4-4),

Equation 13.4-6.

$$\frac{y_p}{1-y_p}=\frac{\alpha^*[x_o-(p_l/p_h)y_p]}{(1-x_o)-(p_l/p_h)(1-y_p)}$$

This equation relates the reject concentration x_o to the permeate concentration y_p. The concentration in the bulk or reject gas phase is x_o. The permeate concentration y_p in the bulk gas phase is the same as the gas concentration y' on the lower-pressure side immediately adjacent to the dense-phase membrane or on the low-pressure side of the dense skin layer of the asymmetric membrane, which is called the interface or local concentration.

Equation (13.4-6) is a quadratic equation and its solution is

Equation 13.4-7.

$$y_p=\frac{-b+\sqrt{b^2-4ac}}{2a}$$

where

$$a=1-\alpha^*,\qquad b=-1+\alpha^*+\frac{1}{r}+\frac{x_o}{r}(\alpha^*-1),\qquad c=\frac{-\alpha^*x_o}{r},\qquad r=p_l/p_h$$

Making an overall material balance on component *A,*

Equation 13.4-8.

$$L_fx_f=L_ox_o+V_py_p$$

Dividing by L_f and solving for the outlet reject composition,

Equation 13.4-9.

$$x_o=\frac{x_f-\theta y_p}{(1-\theta)}\quad\text{or}\quad y_p=\frac{x_f-x_o(1-\theta)}{\theta}$$

Substituting $V_p=\theta L_f$ from Eq. (13.4-2) into Eq. (13.4-3) and solving for the membrane area, A_m,

Equation 13.4-10.

$$A_m=\frac{\theta L_fy_p}{(P'_A/t)(p_hx_o-p_ly_p)}$$

Solution of Equations for Design of Complete-Mixing Case

For design of a system, there are seven variables in the complete-mixing model (H1), x_f, x_o, y_p, θ, α^*, p_l/p_h, and A_m, four of which are independent variables. Two commonly occurring cases are considered here.

Case 1

This is the simplest case, where x_f, x_o, α^*, and p_l/p_h are given and y_p, θ, and A_m are to be determined by solution of the equations. By use of the quadratic equation, Eq. (13.4-7) is solved for the permeate composition y_p in terms of x_o. Hence, to solve this case, y_p is first calculated using Eq. (13.4-7). Then the fraction of feed permeated, θ, is calculated using Eq. (13.4-9) and the membrane area, A_m, using Eq. (13.4-10).

EXAMPLE 13.4-1. Design of a Membrane Unit for Complete Mixing

A membrane is to be used to separate a gaseous mixture of *A* and *B* whose feed flow rate is $L_f = 1 \times 10^4$ cm^3 (STP)/s and feed composition of *A* is $x_f = 0.50$ mole fraction. The desired composition of the reject is $x_o = 0.25$. The membrane thickness $t = 2.54 \times 10^{-3}$ cm, the pressure on the feed side is $p_h = 80$ cm Hg, and on the permeate side it is $p_l = 20$ cm Hg. The permeabilities are $P'_A = 50 \times 10^{-10}$ cm^3 (STP) · cm/(s · cm^2 · cm Hg) and $P'_B = 5 \times 10^{-10}$. Assuming the complete-mixing model, calculate the permeate composition, y_p, the fraction permeated, θ, and the membrane area, A_m.

Solution: Substituting into Eq. (13.4-5),

$$\alpha^* = \frac{P'_A}{P'_B} = \frac{50 \times 10^{-10}}{(5 \times 10^{-10})} = 10$$

Using Eq. (13.4-7),

$$r = p_l/p_h = 20/80 = 0.25$$

$$a = 1 - \alpha^* = 1 - 10 = -9$$

$$b = -1 + \alpha^* + \frac{1}{r} + \frac{x_o}{r}(\alpha^* - 1)$$

$$= -1 + 10 + \frac{1}{0.25} + \frac{0.25}{0.25}(10 - 1) = 22.0$$

$$c = \frac{-\alpha^* x_o}{r} = \frac{-10}{0.25}(0.25) = -10$$

$$y_p = \frac{-b + \sqrt{b^2 - 4ac}}{2a}$$

$$= \frac{-22.0 + \sqrt{(22.0)^2 - 4(-9)(-10)}}{2(-9)} = 0.604$$

Using the material-balance equation (13.4-9),

$$x_o = \frac{x_f - \theta y_p}{1 - \theta}; \qquad 0.25 = \frac{0.50 - \theta(0.604)}{1 - \theta}$$

Solving, $\theta = 0.706$. Also, using Eq. (13.4-10),

$$\begin{aligned} A_m &= \frac{\theta L_f y_p}{(P'_A/t)(p_h x_o - p_l y_p)} \\ &= \frac{0.706(1 \times 10^4)(0.604)}{[50 \times 10^{-10}/(2.54 \times 10^{-3})](80 \times 0.25 - 20 \times 0.604)} \\ &= 2.735 \times 10^8 \text{ cm}^2\ (2.735 \times 10^4 \text{ m}^2) \end{aligned}$$

Case 2

In this case x_f, θ, α^*, and p_l/p_h are given and y_p, x_o, and A_m are to be determined. Equation (13.4-7) cannot be solved for y_p since x_o is unknown. Hence, x_o from Eq. (13.4-9) is substituted into Eq. (13.4-7) and the resulting equation solved for y_p using the quadratic equation, to give

Equation 13.4-11.

$$y_p = \frac{-b_1 + \sqrt{b_1^2 - 4a_1 c_1}}{2a_1}$$

where

$$a_1 = \theta + \frac{p_l}{p_h} - \frac{p_l}{p_h}\theta - \alpha^*\theta - \alpha^*\frac{p_l}{p_h} + \alpha^*\frac{p_l}{p_h}\theta$$

$$b_1 = 1 - \theta - x_f - \frac{p_l}{p_h} + \frac{p_l}{p_h}\theta + \alpha^*\theta + \alpha^*\frac{p_l}{p_h} - \alpha^*\frac{p_l}{p_h}\theta + \alpha^* x_f$$

$$c_1 = -\alpha^* x_f$$

After solving for y_p, the value of x_o is calculated from Eq. (13.4-9) and A_m from Eq. (13.4-10).

EXAMPLE 13.4-2. Membrane Design for Separation of Air

It is desired to determine the membrane area needed to separate an air stream using a membrane 1 mil thick with an oxygen permeability of $P'_A = 500 \times 10^{-10}$ cm^3 (STP) · cm/(s · cm^2 · cm Hg). An $\alpha^* = 10$ for oxygen permeability divided by nitrogen permeability (S6) will be used. The feed rate is $L_f = 1 \times 10^6$ cm^3 (STP)/s and the fraction cut $\theta = 0.20$. The pressures selected for use are $p_h = 190$ cm Hg and $p_l = 19$ cm Hg. Again, assuming the complete-mixing model, calculate the permeate composition, the reject composition, and the area.

Solution: Using Eq. (13.4-11) for a feed composition of $x_f = 0.209$,

$$\begin{aligned} a_1 &= \theta + \frac{p_l}{p_h} - \frac{p_l}{p_h}\theta - \alpha^*\theta - \alpha^*\frac{p_l}{p_h} + \alpha^*\frac{p_l}{p_h}\theta \\ &= 0.2 + \frac{19}{190} - \frac{19}{190}(0.2) - 10(0.2) - 10\frac{(19)}{190} + 10\left(\frac{19}{190}\right)(0.2) = -2.52 \end{aligned}$$

$$\begin{aligned} b_1 &= 1 - \theta - x_f - \frac{p_l}{p_h} + \frac{p_l}{p_h}\theta + \alpha^*\theta + \alpha^*\frac{p_l}{p_h} - \alpha^*\frac{p_l}{p_h}\theta + \alpha^* x_f \\ &= 1 - 0.2 - 0.209 - \frac{19}{190} + \frac{19}{190}(0.2) + 10(0.2) \\ &\quad + 10\left(\frac{19}{190}\right) - 10\left(\frac{19}{190}\right)(0.2) + 10(0.209) = 5.401 \end{aligned}$$

$$c_1 = -\alpha^* x_f = -10(0.209) = -2.09$$

$$y_p = \frac{-b_1 + \sqrt{b_1^2 - 4a_1c_1}}{2a_1}$$

$$= \frac{-5.401 + \sqrt{(5.401)^2 - 4(-2.52)(-2.09)}}{2(-2.52)}$$

$$= 0.5067$$

Substituting into Eq. (13.4-9),

$$x_o = \frac{x_f - \theta y_p}{(1-\theta)} = \frac{0.209 - 0.2(0.5067)}{(1-0.2)} = 0.1346$$

Finally, using Eq. (13.4-10) to find the area,

$$A_m = \frac{\theta L_f y_p}{(P'_A/t)(p_h x_o - p_l y_p)}$$

$$= \frac{0.2(1 \times 10^6)(0.5067)}{(500 \times 10^{-10}/2.54 \times 10^{-3})(190 \times 0.1346 - 19 \times 0.5067)}$$

$$= 3.228 \times 10^8 \text{ cm}^2$$

Minimum Concentration of Reject Stream

If all of the feed is permeated, then $\theta = 1$ and the feed composition $x_f = y_p$. For all values of $\theta < 1$, the permeate composition $y_p > x_f$ (H1). Substituting the value $x_f = y_p$ into Eq. (13.4-7) and solving, the minimum reject composition x_{oM} for a given x_f value is obtained as

Equation 13.4-12.

$$x_{oM} = \frac{x_f\left[1 + (\alpha^* - 1)\dfrac{p_l}{p_h}(1 - x_f)\right]}{\alpha^*(1 - x_f) + x_f}$$

Hence, a feed of x_f concentration cannot be stripped lower than a value of x_{oM} even with an infinitely large membrane area for a completely mixed system. To strip beyond this limiting value, a cascade-type system could be used. However, a single unit which is not completely mixed but is designed for plug flow could also be used.

EXAMPLE 13.4-3. Effect of Feed Composition on Minimum Reject Concentration

Calculate the minimum reject concentration for Example 13.4-1 where the feed concentration is $x_f = 0.50$. Also, what is the effect of raising the feed purity to $x_f = 0.65$?

Solution: Substituting $x_f = 0.50$ into Eq. (13.4-12),

$$x_{oM} = \frac{x_f\left[1 + (\alpha^* - 1)\dfrac{p_l}{p_h}(1 - x_f)\right]}{\alpha^*(1 - x_f) + x_f}$$

$$= \frac{0.50\left[1 + (10 - 1)\left(\dfrac{20}{80}\right)(1 - 0.50)\right]}{10(1 - 0.50) + 0.50}$$

$$= 0.1932$$

For $x_f = 0.65$,

$$x_{oM} = \frac{0.65\left[1 + (10 - 1)\left(\dfrac{20}{80}\right)(1 - 0.65)\right]}{10(1 - 0.65) + 0.65} = 0.2780$$

COMPLETE-MIXING MODEL FOR MULTICOMPONENT MIXTURES

Derivation of Equations

When multicomponent mixtures are present, the iteration method of Stern et al. (S1) is quite useful. This method will be derived for a ternary mixture of components *A, B,* and *C.* The process flow diagram is the same as Fig. 13.4-1, where the feed composition x_f is x_{fA}, x_{fB}, and x_{fC}. The known values are

$$x_{fA}, x_{fB}, x_{fC};\ L_f;\ \theta;\ p_h, p_l;\ P'_A, P'_B, P'_C;\ \text{and } t$$

The unknown values to be determined are

$$y_{pA}, y_{pB}, y_{pC};\ x_{oA}, x_{oB}, x_{oC};\ V_p \text{ or } L_o;\ \text{and } A_m$$

These eight unknowns can be obtained by solving a set of eight simultaneous equations using an iteration method. Three rate-of-permeation equations similar to Eq. (13.4-3) are as follows for components *A, B,* and *C:*

Equation 13.5-1.

$$V_p y_{pA} = \frac{P'_A}{t} A_m (p_h x_{oA} - p_l y_{pA})$$

Equation 13.5-2.

$$V_p y_{pB} = \frac{P'_B}{t} A_m (p_h x_{oB} - p_l y_{pB})$$

Equation 13.5-3.

$$V_p y_{pC} = \frac{P'_C}{t} A_m (p_h x_{oC} - p_l y_{pC})$$

The three material-balance equations similar to Eq. (13.4-9) are written for components *A, B,* and *C:*

Equation 13.5-4.

$$x_{oA} = \frac{1}{1-\theta}x_{fA} - \frac{\theta}{1-\theta}y_{pA}$$

Equation 13.5-5.

$$x_{oB} = \frac{1}{1-\theta}x_{fB} - \frac{\theta}{1-\theta}y_{pB}$$

Equation 13.5-6.

$$x_{oC} = \frac{1}{1-\theta}x_{fC} - \frac{\theta}{1-\theta}y_{pC}$$

Also, two final equations can be written as

Equation 13.5-7.

$$\sum_n y_{pn} = y_{pA} + y_{pB} + y_{pC} = 1.0$$

Equation 13.5-8.

$$\sum_n x_{on} = x_{oA} + x_{oB} + x_{oC} = 1.0$$

Substituting x_{oA} from Eq. (13.5-4) into Eq. (13.5-1) and solving for A_m,

Equation 13.5-9.

$$A_m = \frac{V_p y_{pA} t}{P'_A\left[\frac{p_h}{1-\theta}(x_{fA} - \theta y_{pA}) - p_l y_{pA}\right]}$$

For component *B,* Eq. (13.5-5) is substituted into Eq. (13.5-2), giving

Equation 13.5-10.

$$A_m = \frac{V_p y_{pB} t}{P'_B\left[\frac{p_h}{1-\theta}(x_{fB} - \theta y_{pB}) - p_l y_{pB}\right]}$$

Rearranging Eq. (13.5-10) and solving for y_{pB},

Equation 13.5-11.

$$y_{pB} = \frac{p_h x_{fB}/(1-\theta)}{V_p t/(P'_B A_m) + \theta p_h/(1-\theta) + p_l}$$

In a similar manner Eq. (13.5-12) is derived for y_{pC}:

Equation 13.5-12.

$$y_{pC} = \frac{p_h x_{fC}/(1-\theta)}{V_p t/(P'_C A_m) + \theta p_h/(1-\theta) + p_l}$$

Iteration Solution Procedure for Multicomponent Mixtures

The following iteration or trial-and-error procedure can be used to solve the equations above:

1. A value of y_{pA} is assumed where $y_{pA} > x_{fA}$.
2. Using Eq. (13.4-2) and the known value of θ, V_p is calculated.
3. The membrane area is calculated from Eq. (13.5-9).
4. Values of y_{pB} and y_{pC} are calculated from Eqs. (13.5-11) and (13.5-12).
5. The sum $\Sigma_n y_{pn}$ is calculated from Eq. (13.5-7). If this sum is not equal to 1.0. steps 1 through 5 are repeated until the sum is 1.0.
6. Finally, x_{oA}, x_{oB}, and x_{oC} are calculated from Eqs. (13.5-4), (13.5-5), and (13.5-6).

EXAMPLE 13.5-1. Design of Membrane Unit for Multicomponent Mixture

A multicomponent gaseous mixture having a composition of $x_{fA} = 0.25$, $x_{fB} = 0.55$, and $x_{fC} = 0.20$ is to be separated by a membrane with a thickness of 2.54×10^{-3} cm using the complete-mixing model. The feed flow rate is 1.0×10^4 cm^3 (STP)/s and the permeabilities are $P'_A = 200 \times 10^{-10}$ cm^3 (STP) · cm/(s · cm^2 · cm Hg), $P'_B = 50 \times 10^{-10}$, and $P'_C = 25 \times 10^{-10}$. The pressure on the feed side is 300 cm Hg and 30 cm Hg on the permeate side. The fraction permeated will be 0.25. Calculate the permeate composition, reject composition, and membrane area using the complete-mixing model.

Solution: Following the iteration procedure, a value of $y_{pA} = 0.50$ is assumed. Substituting into Eq. (13.4-2) for step 2,

$$V_p = \theta L_f = 0.25 \times 1.0 \times 10^4 = 0.25 \times 10^4 \text{ cm}^3 \text{ (STP)/s}$$

Using Eq. (13.5-9), the membrane area for step (3) is

$$A_m = \frac{V_p y_{pA} t}{P'_A\left[\frac{p_h}{1-\theta}(x_{fA} - \theta y_{pA}) - p_l y_{pA}\right]}$$

$$= \frac{0.25 \times 10^4 (0.50)(2.54 \times 10^{-3})}{200 \times 10^{-10}} \Bigg/ \left[\frac{300}{1-0.25}(0.25 - 0.25 \times 0.50) - 30(0.50)\right]$$

$$= 4.536 \times 10^6 \text{ cm}^2$$

Following step 4, the values y_{pB} and y_{pC} are calculated using Eqs. (13.5-11) and (13.5-12):

$$y_{pB} = \frac{p_h x_{fB}/(1-\theta)}{V_p t/(P'_B A_m) + \theta p_h/(1-\theta) + p_l}$$

$$= \frac{300 \times 0.55/(1-0.25)}{0.25 \times 10^4 \times 2.54 \times 10^{-3}/(50 \times 10^{-10} \times 4.536 \times 10^6) + 0.25 \times 300/(1-0.25) + 30}$$

$$= 0.5366$$

$$
\begin{aligned}
y_{pC} &= \frac{p_h x_{fC}/(1-\theta)}{V_p t/(P'_C A_m) + \theta p_h/(1-\theta) + p_l} \\
&= \frac{300 \times 0.20/(1-0.25)}{0.25 \times 10^4 \times 2.54 \times 10^{-3}/(25 \times 10^{-10} \times 4.536 \times 10^6) + 0.25 \times 300/(1-0.25) + 30} \\
&= 0.1159
\end{aligned}
$$

Substituting into Eq. (13.5-7),

$$\sum_n y_{pn} = y_{pA} + y_{pB} + y_{pC} = 0.5000 + 0.5366 + 0.1159 = 1.1525$$

For the second iteration, assuming that $y_{pA} = 0.45$, the following values are calculated:

$$A_m = 3.546 \times 10^6 \text{ cm}^2 \qquad y_{pB} = 0.4410 \qquad y_{pC} = 0.0922$$

$$\sum_n y_{pn} = 0.9832$$

The final iteration values are $A_m = 3.536 \times 10^6$ cm^2; $y_{pA} = 0.4555$, $y_{pB} = 0.4502$, and $y_{pC} = 0.0943$. Substituting into Eqs. (13.5-4), (13.5-5), and (13.5-6),

$$
\begin{aligned}
x_{oA} &= \frac{1}{1-\theta} x_{fA} - \frac{\theta}{1-\theta} y_{pA} = \frac{1}{1-0.25}(0.25) \\
&\quad - \frac{0.25}{1-0.25}(0.4555) = 0.1815 \\
x_{oB} &= \frac{1}{1-\theta} x_{fB} - \frac{\theta}{1-\theta} y_{pB} = \frac{1}{1-0.25}(0.55) \\
&\quad - \frac{0.25}{1-0.25}(0.4502) = 0.5833 \\
x_{oC} &= \frac{1}{1-\theta} x_{fC} - \frac{\theta}{1-\theta} y_{pC} = \frac{1}{1-0.25}(0.20) \\
&\quad - \frac{0.25}{1-0.25}(0.0943) = 0.2352
\end{aligned}
$$

CROSS-FLOW MODEL FOR GAS SEPARATION BY MEMBRANES

Derivation of Basic Equations

A detailed flow diagram for the cross-flow model derived by Weller and Steiner (W3, W4) is shown in Fig. 13.6-1. In this case the longitudinal velocity of the high-pressure or reject stream is large enough that this gas stream is in plug flow and flows parallel to the membrane. On the low-pressure side the permeate stream is almost pulled into vacuum, so that the flow is essentially perpendicular to the membrane.

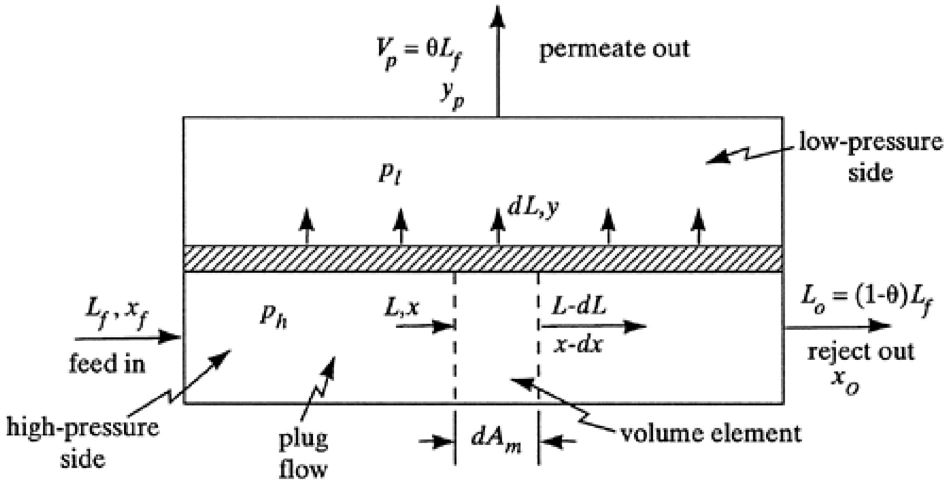

Figure 13.6-1. Process flow diagram for cross-flow model.

This model assumes no mixing in the permeate side as well as no mixing on the high-pressure side. Hence, the permeate composition at any point along the membrane is determined by the relative rates of permeation of the feed components at that point. This cross-flow pattern approximates that in an actual spiral-wound membrane separator (Fig. 13.3-1) with a high-flux asymmetric membrane resting on a porous felt support (P2, R1).

Referring to Fig. 13.6-1, the local permeation rate over a differential membrane area dA_m at any point in the stage is

Equation 13.6-1.

$$y\,dV = \frac{P'_A}{t}[p_h x - p_l y]\,dA_m$$

Equation 13.6-2.

$$(1-y)\,dV = \frac{P'_B}{t}[p_h(1-x) - p_l(1-y)]\,dA_m$$

where $dL = dV$ and is the total flow rate permeating through the area dA_m. Dividing Eq. (13.6-1) by (13.6-2) gives

Equation 13.6-3.

$$\frac{y}{1-y} = \frac{\alpha^*[x-(p_l/p_h)y]}{(1-x)-(p_l/p_h)(1-y)}$$

This equation relates the permeate composition y to the reject composition x at a point along the path. It is similar to Eq. (13.4-6) for complete mixing. Hwang and Kammermeyer (**H1**) give a computer program for the solution of the above system of differential equations by numerical methods.

Weller and Steiner (W3, W4) used some ingenious transformations and were able to obtain an analytical solution to the three equations as follows:

Equation 13.6-4.

$$\frac{(1-\theta^*)(1-x)}{(1-x_f)} = \left(\frac{u_f - E/D}{u - E/D}\right)^R \left(\frac{u_f - \alpha^* + F}{u - \alpha^* + F}\right)^S \left(\frac{u_f - F}{u - F}\right)^T$$

where

$$\theta^* = 1 - \frac{L}{L_f}$$

$$i = \frac{x}{1 - x}$$

$$u = -Di + (D^2 i^2 + 2Ei + F^2)^{0.5}$$

$$D = 0.5\left[\frac{(1 - \alpha^*)p_l}{p_h} + \alpha^*\right]$$

$$E = \frac{\alpha^*}{2} - DF$$

$$F = -0.5\left[\frac{(1 - \alpha^*)p_l}{p_h} - 1\right]$$

$$R = \frac{1}{2D - 1}$$

$$S = \frac{\alpha^*(D - 1) + F}{(2D - 1)(\alpha^*/2 - F)}$$

$$T = \frac{1}{1 - D - (E/F)}$$

The term u_f is the value of u at $i = i_f = x_f/(1 - x_f)$. The value of θ^* is the fraction permeated up to the value of x in Fig. 13.6-1. At the outlet where $x = x_0$, the value of θ^* is equal to θ, the total fraction permeated. The composition of the exit permeate stream is y_p and is calculated from the overall material balance, Eq. (13.4-9).

The total membrane area was obtained by Weller and Steiner (W3, W4) using some additional transformations of Eqs. (13.6-1)-(13.6-3) to give

Equation 13.6-5.

$$A_m = \frac{tL_f}{p_h P'_B} \int_{i_0}^{i_f} \frac{(1 - \theta^*)(1 - x)\,di}{(f_i - i)\left[\frac{1}{1 + i} - \frac{p_l}{p_h}\left(\frac{1}{1 + f_i}\right)\right]}$$

where

$$f_i = (Di - F) + (D^2 i^2 + 2Ei + F^2)^{0.5}$$

Values of θ^* in the integral can be obtained from Eq. (13.6-4). The integral can be calculated numerically. The term i_f is the value of i at the feed x_f, and i_o is the value of i at the outlet x_o. A shortcut approximation of the area without using a numerical integration, available from Weller and Steiner (W3), has a maximum error of about 20%.

Procedure for Design of Cross-Flow Case

In the design for the complete-mixing model there are seven variables, and two of the most common cases were discussed in Section 13.4B. Similarly, for the cross-flow model these same common cases occur.

Case 1

The values of x_f, x_o, α^*, and p_l/p_h are given and y_p, θ and A_m are to be determined. The value of θ^* or θ can be calculated directly from Eq. (13.6-4) since all other values in this equation are known. Then y_p is calculated from Eq. (13.4-9). To calculate the area A_m, a series of values of x less than the feed x_f and greater than the reject outlet x_o are substituted into Eq. (13.6-4) to give a series of θ^* values. These values are then used to numerically or graphically integrate Eq. (13.6-5) to obtain the area A_m.

Case 2

In this case the values of x_f, θ, α^*, and p_l/p_h are given and y_p, x_o, and A_m are to be determined. This is trial and error, where values of x_o are substituted into Eq. (13.6-4) to solve the equation. The membrane area is calculated as in Case 1.

EXAMPLE 13.6-1. Design of a Membrane Unit Using Cross-Flow

The same conditions for the separation of an air stream as given in Example 13.4-2 for complete mixing are to be used in this example. The process flow streams will be in cross-flow. The given values are $x_f = 0.209$, $\theta = 0.20$, $a^* = 10$, $p_h = 190$ cm Hg, $p_l = 19$ cm Hg, $L_f = 1 \times 10^6$ cm^3 (STP)/s, $P'_A = 500 \times 10^{-10}$ cm^3 (STP) · cm/(s · cm^2 · cm Hg), and $t = 2.54 \times 10^{-3}$ cm. Do as follows:

a. Calculate y_p, x_o, and A_m.
b. Compare the results with Example 13.4-2.

Solution: Since this is the same as Case 2, a value of $x_o = 0.1642$ will be used for the first trial for part (a). Substituting into Eq. (13.6-4),

$$i = i_f = \frac{x_f}{1 - x_f} = \frac{0.209}{1 - 0.209} = 0.2642$$

$$i = \frac{0.1642}{1 - 0.1642} = 0.1965$$

$$D = 0.5\left[\frac{(1 - \alpha^*)p_l}{p_h} + \alpha^*\right]$$

$$= 0.5\left[\frac{(1 - 10)19}{190} + 10\right] = 4.550$$

$$F = -0.5\left[\frac{(1 - \alpha^*)p_l}{p_h} - 1\right]$$

$$= -0.5\left[\frac{(1 - 10)19}{190} - 1\right] = 0.950$$

$$E = \frac{\alpha^*}{2} - DF = \frac{10}{2} - 4.550(0.950) = 0.6775$$

$$R = \frac{1}{2D - 1} = \frac{1}{2(4.550) - 1} = 0.12346$$

$$S = \frac{\alpha^*(D - 1) + F}{(2D - 1)(\alpha^*/2 - F)}$$

$$= \frac{10(4.550 - 1) + 0.950}{(2 \times 4.550 - 1)(10/2 - 0.950)} = 1.1111$$

$$T = \frac{1}{1 - D - (E/F)}$$

$$= \frac{1}{1 - 4.550 - 0.6775/0.950} = -0.2346$$

$$u_f = -Di + (D^2i^2 + 2Ei + F^2)^{0.5}$$

$$= -(4.550)(0.2642) + [(4.550)^2(0.2642)^2 + 2(0.6775)(0.2642) + (0.950)^2]^{0.5}$$

$$= 0.4427$$

$$u = -(4.550)(0.1965) + [(4.550)^2(0.1965)^2 + 2(0.6775)(0.1965) + (0.950)^2]^{0.5}$$

$$= 0.5089$$

$$\frac{(1-\theta^*)(1-x)}{(1-x_f)} = \frac{(1-\theta^*)(1-0.1642)}{(1-0.209)}$$

$$= \left(\frac{0.4427 - 0.6775/4.550}{0.5089 - 0.6775/4.550}\right)^{0.12346} \times \left(\frac{0.4427 - 10 + 0.950}{0.5089 - 10 + 0.950}\right)^{1.1111} \times \left(\frac{0.4427 - 0.950}{0.5089 - 0.950}\right)^{-0.2346}$$

Solving, $\theta^* = 0.0992$. This value of 0.0992 does not agree with the given value of $\theta = 0.200$. However, these values can be used later to solve Eq. (13.6-5).

For the second iteration, a value of $x_o = 0.142$ is assumed and is used again to solve for θ^* in Eq. (13.6-4), which results in $\theta^* = 0.1482$. For the final iteration, $x_o = 0.1190$ and $\theta^* = \theta = 0.2000$. Several more values are calculated for later use and are: for x_o = 0.187, θ^* = 0.04876, and for x_o = 0.209, θ^* = 0. These values are tabulated in Table 13.6-1.

Table 13.6-1. Calculated Values for Example 13.6-1

θ^*	x	y_p	F_t
0	**0.209**	**0.6550**	**0.6404**
0.04876	**0.1870**	**0.6383**	**0.7192**
0.0992	**0.1642**	**0.6158**	**0.8246**
0.1482	**0.1420**	**0.5940**	**0.9603**
0.2000	**0.1190**	**0.5690**	**1.1520**

Using the material-balance equation (13.4-9) to calculate y_p,

$$y_p = \frac{x_f - x_o(1-\theta)}{\theta} = \frac{0.209 - 0.1190(1 - 0.2000)}{0.2000} = 0.5690$$

To calculate y_p at $\theta^* = 0$, Eqs. (13.6-3) and (13.4-17) must be used, giving $y_p = 0.6550$.

To solve for the area, Eq. (13.6-5) can be written as

Equation 13.6-6.

$$A_m = \frac{tL_f}{p_h P'_B}\int_{i_o}^{i_f}\left[\frac{(1-\theta^*)(1-x)}{(f_i - i)\left[\frac{1}{1+i} - \frac{p_l}{p_h}\left(\frac{1}{1+f_i}\right)\right]}\right]di = \frac{tL_f}{p_h P'_B}\int_{i_o}^{i_f} F_i\, di$$

where the function F_i is defined as above. Values of F_i will be calculated for different values of i in order to integrate the equation. For $\theta^* = 0.200$, $x_o = 0.119$, and from Eq. (13.6-4),

$$i = i_o = \frac{x}{(1-x)} = \frac{0.119}{(1-0.119)} = 0.1351$$

From Eq. (13.6-5),

$$\begin{aligned} f_i &= (Di - F) + (D^2i^2 + 2Ei + F^2)^{0.5} \\ &= (4.55 \times 0.1351 - 0.950) + [(4.55)^2(0.1351)^2 \\ &\quad + 2(0.6775)(0.1351) + (0.95)^2]^{0.5} \\ &= 0.8744 \end{aligned}$$

Using the definition of F_i from Eq. (13.6-6),

$$\begin{aligned} F_i &= \frac{(1-\theta^*)(1-x)}{(f_i - i)\left[\frac{1}{1+i} - \frac{p_l}{p_h}\left(\frac{1}{1+f_i}\right)\right]} \\ &= \frac{(1-0.200)(1-0.119)}{(0.8744 - 0.1351)\left[\frac{1}{1+0.1351} - \frac{19}{190}\left(\frac{1}{1+0.8744}\right)\right]} \\ &= 1.1520 \end{aligned}$$

Other values of F_i *are* calculated for the remaining values of θ^* and are tabulated in Table 13.6-1. The integral of Eq. (13.6-6) is obtained by using the values from Table 13.6-1 and numerically integrating F_i versus i to give an area of 0.1082. Finally, substituting into Eq. (13.6-6),

$$\begin{aligned} A_m &= \frac{tL_f}{p_h P'_B}\int_{i_o}^{i_f} F_i\, di = \frac{2.54 \times 10^{-3}(1 \times 10^6)}{190(50 \times 10^{-10})/10}(0.1082) \\ &= 2.893 \times 10^8\ \text{cm}^2 \end{aligned}$$

For part (b), from Example 13.4-2, $y_p = 0.5067$ and $A_m = 3.228 \times 10^8$ cm^2. Hence, the cross-flow model yields a higher y_p of 0.5690, compared to 0.5067 for the complete-mixing model. Also, the area for the cross-flow model is 10% less than for the complete-mixing model.

DERIVATION OF EQUATIONS FOR COUNTERCURRENT AND COCURRENT FLOW FOR GAS SEPARATION FOR MEMBRANES

Concentration Gradients in Membranes

Dense-phase membrane

In gas separation using a dense-phase symmetrical polymer membrane, the solute diffuses through the high-pressure-side gas film to the membrane surface. Then it dissolves in the membrane. At the interface equilibrium occurs. The solute then diffuses through the solid membrane, and finally diffuses through the gas film. The gas film resistances are quite small and can be neglected (*N1*). In Fig. 13.7-1a the concentration profiles are shown. The concentration y in the flowing bulk gas phase is the same as y at the interface of the dense polymer and depends on the flow pattern of the permeate phase.

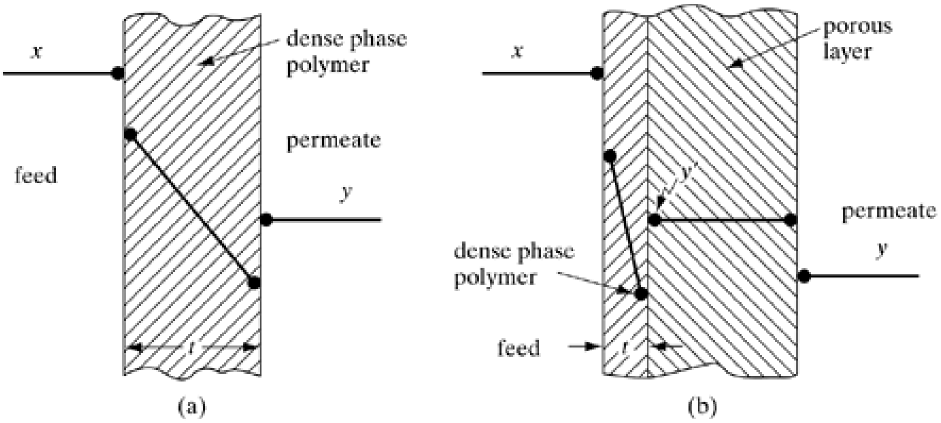

Figure 13.7-1. Concentration profiles in membranes. (a) dense-phase symmetrical membranes, (b) asymmetric membrane.

Asymmetric membrane

As shown in Fig. 13.7-1b, the membrane includes a very thin, dense polymer membrane which is about 0.1 to 1 μm thick (M5, P7) and a very thick porous layer 50–200 μm thick. A typical hollow-fiber membrane for air separation has an ID of 95 μm and an OD of 135 μm, with a wall thickness of 20 μm.

The concentration gradient in the thin dense polymer phase is similar to that for the symmetrical membrane. However, the concentration *y of component A* in the bulk permeate gas phase is not the same as y' at the surface of the thin dense polymer layer. The concentration y of the bulk gas permeate stream depends on the flow pattern and material balances. Also, the value of y can be greater or less than y'.

The porous layer is so open that there is assumed to be little or no resistance to the flow and y' is constant along this path. Hence, it is assumed that there is no penetration or mixing of the bulk gas phase y inside the porous layer.

Derivation of Equations for Countercurrent Flow in Dense-Phase Symmetric Membranes

A flow diagram for this countercurrent-flow model is given in Fig. 13.7-2, where both streams are in plug flow. The derivation follows that given by others (B1, N1, P4, W5).

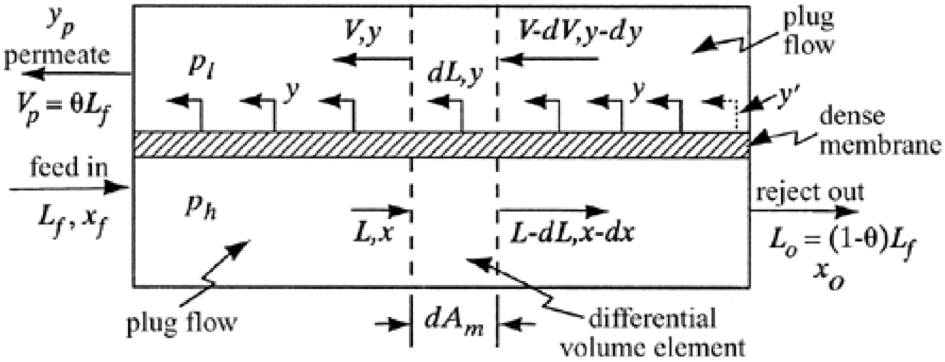

Figure 13.7-2. Flow diagram for the countercurrent-flow model with dense-phase symmetric membrane.

Making a total material balance,

Equation 13.7-1.

$$L_f = L_o + V_p$$

where L_f is total feed flow rate, cm^3 (STP)/s, L_o is outlet nonpermeate (reject) flow rate, cm^3 (STP)/s, and V_p is outlet permeate flow rate, cm^3 (STP)/s. The rates of permeation of *A* and in *B* in a binary mixture are similar to Eqs. (13.4-3) and (13.4-4):

Equation 13.7-2.

$$V_A/A_m = Vy/A_m = (P'_A/t)(p_h x - p_l y)$$

Equation 13.7-3.

$$V_B/A_m = V(1-y)/A_m = (P'_B/t)[p_h(1-x) - p_l(1-y)]$$

where P'_A is permeability of *A,* cm^3 (STP) · cm/(s · cm^2 · cm Hg); V_A is flow rate of *A* in permeate, cm^3 (STP)/s; A_m is membrane area, cm^2; p_h is total pressure in the high-pressure side, cm Hg; and p_t is total pressure in low-pressure side, cm Hg.

The flux of *A* out of the element with area dA_m is

Equation 13.7-4.

$$dL_A = y\,dL = (P'_A/t)[p_h x - p_l y]\,dA_m$$

The flux of *B* is

Equation 13.7-5.

$$dL_B = (1-y)dL = (P'_B/t)[p_h(1-x) - p_l(1-y)]\,dA_m$$

Making a total balance on the reject stream for area dA_m,

Equation 13.7-6.

$$L = L - dL + dL_A + dL_B$$

This gives

Equation 13.7-7.

$$dL = dL_A + dL_B$$

Making a balance on A for area dA_m,

Equation 13.7-8.

$$Lx = (L - dL)(x - dx) + dL_A$$

Rearranging,

Equation 13.7-9.

$$dL_A = L\,dx + x\,dL$$

Substituting Eq. (13.7-7) into (13.7-9),

Equation 13.7-10.

$$L\,dx = (1 - x)\,dL_A - x\,dL_B$$

Making a total balance on permeate stream for area dA_m,

Equation 13.7-11.

$$V = V - dV + dL_A + dL_B$$

This gives

Equation 13.7-12.

$$dV = dL_A + dL_B$$

Making a balance on A for area dA_m,

Equation 13.7-13.

$$Vy = (V - dV)(y - dy) + dL_A$$

Rearranging,

Equation 13.7-14.

$$dL_A = V\,dy + y\,dV$$

Substituting Eq. (13.7-12) into (13.7-14),

Equation 13.7-15.

$$V\,dy = (1 - y)\,dL_A - y\,dL_B$$

To eliminate the variables L and V, an overall balance is made for the area dA_m and the reject outlet stream:

Equation 13.7-16.

$$L = L_o + V$$

Equation 13.7-17.

$$Lx = L_o x_o + Vy$$

To eliminate *V*, *V* from Eq. (13.7-16) is substituted into (13.7-17) and solved for *L*:

Equation 13.7-18.

$$L = L_o(x_o - y)/(x - y)$$

To eliminate *L*, *L* from Eq. (13.7-16) is substituted into (13.7-17) and solved for *V:*

Equation 13.7-19.

$$V = L_o(x_o - x)/(x - y)$$

Substituting Eq. (13.7-18) into (13.7-10),

Equation 13.7-20.

$$\frac{L_o(x_o - y)\,dx}{(x - y)} = (1 - x)\,dL_A - x\,dL_B$$

Substituting Eqs. (13.7-4) and (13.7-5) into (13.7-20),

Equation 13.7-21.

$$\begin{aligned}\frac{L_o(x_o - y)\,dx}{(x - y)} &= (1 - x)[(P'_A/t)(p_h x - p_l y)]\,dA_m \\ &\quad - x(P'_B/t)[p_h(1 - x) - p_l(1 - y)]\,dA_m\end{aligned}$$

Rearranging,

Equation 13.7-22.

$$\frac{L_o}{(P'_B/t)p_h}\,\frac{dx}{dA_m} = -\left(\frac{x - y}{y - x_o}\right)\{(1 - x)\alpha^*(x - ry) - x[(1 - x) - r(1 - y)]\}$$

where $r = p_l/p_h$ and $\alpha^* = (P'_A/t)/(P'_B/t)$.

In a similar manner, substituting Eq. (13.7-19) into (13.7-15),

Equation 13.7-23.

$$\frac{L_o(x_o - x)\,dy}{(x - y)} = (1 - y)\,dL_A - y\,dL_B$$

Again, substituting Eqs. (13.7-4) and (13.7-5) into (13.7-23) and rearranging,

Equation 13.7-24.

$$\frac{L_o}{(P'_B/t)p_h}\,\frac{dy}{dA_m} = -\left(\frac{x - y}{x - x_o}\right)\{(1 - y)\alpha^*(x - ry) - y[(1 - x) - r(1 - y)]\}$$

Dividing Eq. (13.7-24) by (13.7-22),

Equation 13.7-25.

$$\frac{dy}{dx} = \frac{(y - x_o)}{(x - x_o)} \frac{\{(1 - y)\alpha^*(x - ry) - y[(1 - x) - r(1 - y)]\}}{\{(1 - x)\alpha^*(x - ry) - x[(1 - x) - r(1 - y)]\}}$$

Inverting Eq. (13.7-22),

Equation 13.7-26.

$$\frac{dA_m}{dx} = \frac{-L_o}{(P'_B/t)p_h} \frac{[(y - x_o)/(x - y)]}{\{(1 - y)\alpha^*(x - ry) - x[(1 - x) - r(1 - y)]\}}$$

Solution of Countercurrent Flow Equations in Dense-Phase Symmetric Membranes

At the outlet of the residue stream of composition x_o, the permeate y' and x_o are related by Eq. (13.4-6), repeated here as Eq. (13.7-27), where $y_p = y'$:

Equation 13.7-27.

$$\frac{y'}{1 - y'} = \frac{\alpha^*[x_o - (p_l/p_h)y']}{(1 - x_o) - (p_l/p_h)(1 - y')}$$

The solution to this quadratic equation is given as Eq. (13.4-7).

In order to solve Eqs. (13.7-25) and (13.7-26), the following procedure can be used, where x_o is known or set:

1. Using Eq. (13.7-27), the value of y' is calculated for $x = x_o$.
2. To integrate Eq. (13.7-25), the value of (dy/dx) at $x = x_o$ must be calculated. However, this value is indeterminate since the denominator is zero. Using L'Hopital's rule (N1, P4, R1) the numerator is differentiated with respect to x and the denominator with respect to x and the value of y is set as y' to give

   Equation 13.7-28.

   $$\left(\frac{dy}{dx}\right)_{x=x_o} = \frac{(y' - x_o)[\alpha^* - (\alpha^* - 1)y']}{\{\alpha^*(1 - x_o)(x_o - ry') - x_o[(1 - x_o) - r(1 - y')] - (y' - x_o)[(\alpha^* - 1)(2ry' - x_o - r) - 1]\}}$$

3. Starting at the residual end at x_o, Eq. (13.7-25) is integrated numerically to give the y-versus-x relationship and y_p (P4, R1).
4. The relationship of y versus x is substituted into Eq. (13.7-26), which is integrated from x_f to x_o to obtain the area A_m.
5. Substituting into the material-balance Eqs. (13.4-8) and (13.4-2), the cut or fraction of feed permeated, θ, is calculated (N1, Rl, W5).
6. If θ is set and x_o is unknown, the solution is trial and error. The value of x_o is assumed and the integration of Eq. (13.7-25) is performed to obtain y_p. Then x_o is calculated from Eq. (13.4-9). This is repeated until the assumed and calculated values of x_o agree.

Derivation of Equations for Countercurrent Flow in Asymmetric Membranes

The flow diagram for this countercurrent-flow model is shown in Fig. 13.7-3, where both streams are in plug flow. The permeate y' leaving the membrane differs from the symmetric-membrane case and is not the same as the bulk phase concentration y at this point. This is also shown in Fig. 13.7-1b.

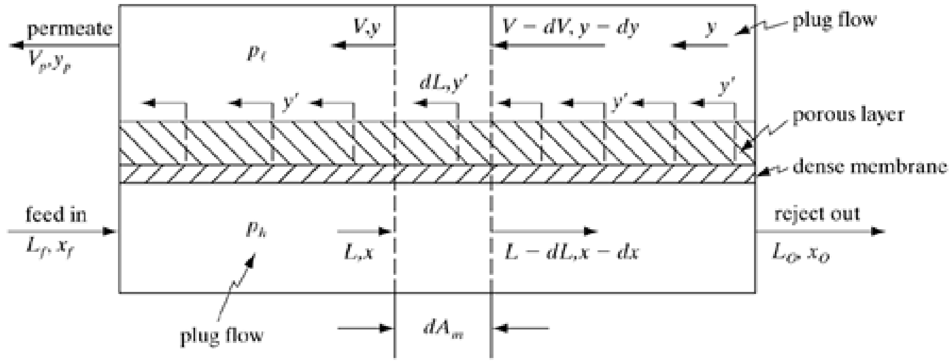

Figure 13.7-3. Flow diagram for countercurrent flow with asymmetric membrane.

The flux of A out of the element with area dA_m is

Equation 13.7-29.

$$dL_A = y\,dL = (P'_A/t)(p_h x - p_l y')\,dA_m$$

where y' is given by Eq. (13.7-30), which is similar to Eqs. (13.7-27) and (13.4-6):

Equation 13.7-30.

$$\frac{y'}{1-y'} = \frac{\alpha^*[x - (p_l/p_h)y']}{(1-x) - (p_l/p_h)(1-y')}$$

The flux of B is

Equation 13.7-31.

$$dL_B = (1-y)\,dL = (P'_B/t)[p_h(1-x) - p_l(1-y')]\,dA_m$$

Equations (13.7-29) and (13.7-31) differ from Eqs. (13.7-4) and (13.7-5) for the symmetric membrane in that y' is used instead of y in the terms for concentration difference.

The rest of the derivation is identical to that for the dense-phase symmetric membrane (N1, R1). The final equations are

Equation 13.7-32.

$$\frac{L_o}{(P'_B/t)p_h}\,\frac{dx}{dA_m} = \frac{-(x-y)}{(y-x_o)}\{(1-x)\alpha^*(x-ry') - x[(1-x) - r(1-y')]\}$$

Equation 13.7-33.

$$\frac{dx}{dy} = \frac{(y-x_o)}{(x-x_o)}\,\frac{\{(1-y)\alpha^*(x-ry') - y[(1-x) - r(1-y')]\}}{\{(1-x)\alpha^*(x-ry') - x[(1-x) - r(1-y')]\}}$$

Inverting Eq. (13.7-32),

Equation 13.7-34.

$$\frac{dA_m}{dx} = \frac{-L_o}{(P'_B/t)p_h}\,\frac{[(y-x_o)/(x-y)]}{\{(1-x)\alpha^*(x-ry') - x[(1-x) - r(1-y')]\}}$$

Equations (13.7-27) for y' and (13.7-28) for (dy/dx) at $x = x_o$ for symmetric membranes are also applicable here for asymmetric membranes. The method of solution for the above equations is similar to that for symmetric membranes.

Derivation of Equations for Cocurrent Flow in Asymmetric Membranes

For cocurrent flow, the cocurrent model is shown in Fig. 13.7-4. The derivation uses Eqs. (13.7-29)-(13.7-31) as before. Proceeding in a manner similar to the countercurrent case, the final equations are (N1, P4, R1):

Equation 13.7-35.

$$\frac{dy}{dx} = \frac{(y - x_f)}{(x - x_f)} \frac{\{(1 - y)\alpha^*(x - ry') - y[(1 - x) - r(1 - y')]\}}{\{(1 - x)\alpha^*(x - ry') - x[(1 - x) - r(1 - y')]\}}$$

Equation 13.7-36.

$$\frac{dA_m}{dx} = \frac{L_f}{(P'_B/t)p_h} \frac{[(y - x_f)/(x - y)]}{\{(1 - x)\alpha^*(x - ry') - x[(1 - x) - r(1 - y')]\}}$$

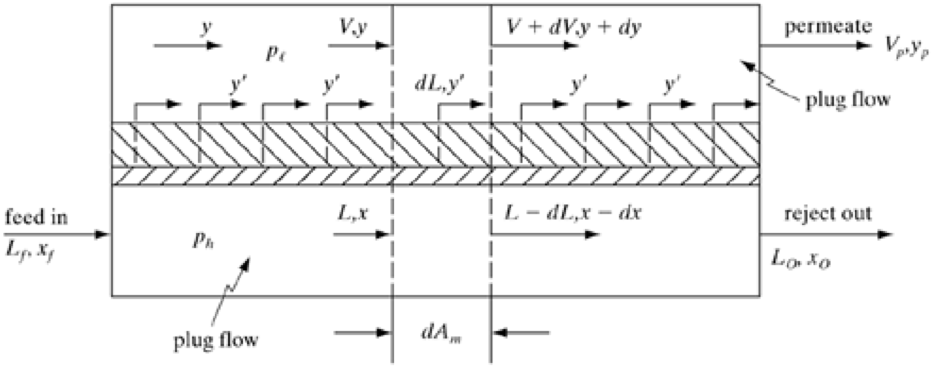

Figure 13.7-4. Flow diagram for cocurrent flow with asymmetric membrane.

The method of solution is similar to that for countercurrent flow. Integration of Eq. (13.7-35) is started at the feed inlet, where y' is determined by using x_f instead of x_o in Eq. (13.7-27). Then, using Eq. (13.7-28) with x_f instead of x_o, (dy/dx) at $x = x_f$ *is* calculated. This is then used to integrate Eq. (13.7-35) starting at the feed end, where $x = x_f$. Finally, Eq. (13.7-36) is integrated to obtain A_m.

Effects of Processing Variables on Gas Separation

Effects of pressure ratio and separation factor on recovery

Using the Weller-Steiner Eq. (13.4-6) for the complete-mixing model, the effects of pressure ratio, p_h/p_l, and separation factor, α*, on permeate purity can be determined for a fixed feed composition. Figure 13.7-5 is a plot of this equation for a feed concentration of 30% (S7). For symmetric and asymmetric membranes, this equation can be expected to provide estimates of product purity and trends for conditions of low to modest recovery in all types of models, including complete-mixing, cross-flow, and countercurrent.

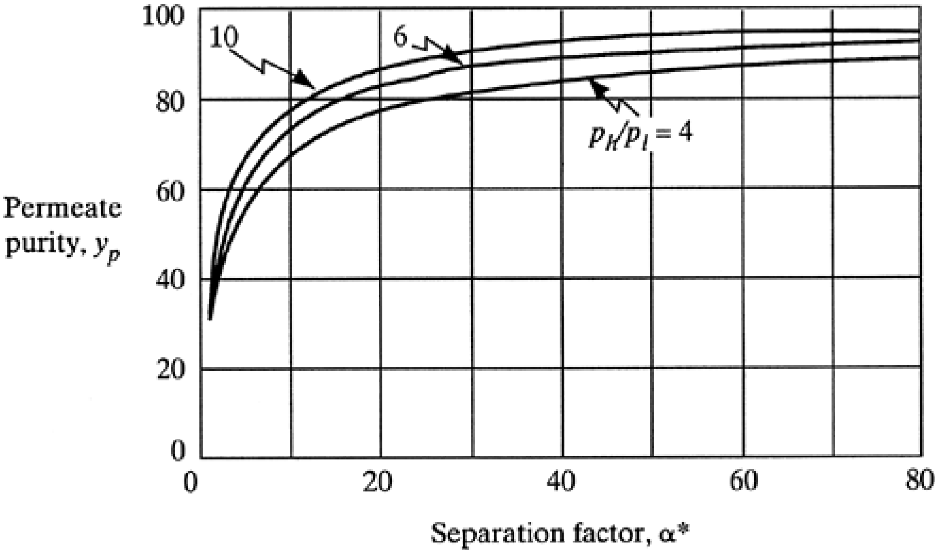

*Figure 13.7-5. Effects of separation factor and pressure ratio on permeate purity. (Feed $x_f = 0.30$.) [From "Membranes Separate Gases Selectively," by D. J. Stookey, C. J. Patton, and G. L. Malcolm, Chem. Eng. Progr., **82**(11), 36(1986). Reproduced by permission of the American Institute of Chemical Engineers.]*

Figure 13.7-5 shows that above an a* of 20, the product purity is not greatly affected. Also, above a pressure ratio of about 6, this ratio has a diminishing effect on product purity.

If liquids are present in the gas separation process, a liquid film can increase the membrane resistance markedly. Liquids can also damage the membrane by chemical action or by swelling or softening. If water vapor is present in the gas streams, the dew point may be reached in the residue product and liquid may condense. Condensation of hydrocarbons must also be avoided.

Effects of process flow patterns on separation in symmetric membranes

Detailed parametric studies have been done by various investigators (P4, P5, W5) for binary systems. They compared the four flow patterns of complete mixing, cross-flow, cocurrent, and countercurrent flow. In Fig. 13.7-6 (W5) the permeate concentration is shown plotted versus stage cut, θ, for a feed of air ($x_f = 0.209$ for oxygen) with α* = 10 and $p_h/p_l = 5$. It is shown that, as expected, the countercurrent flow pattern gives the best separation. The other patterns—cross-flow, cocurrent, and complete mixing—give lower separations in descending order. Note that when the stage cut $\theta = 0$, all flow patterns are equivalent to the complete mixing model and give the same permeate composition. Also, at $\theta = 1.00$, all patterns again give the same value of $y_p = 0.209$, which is also the feed composition.

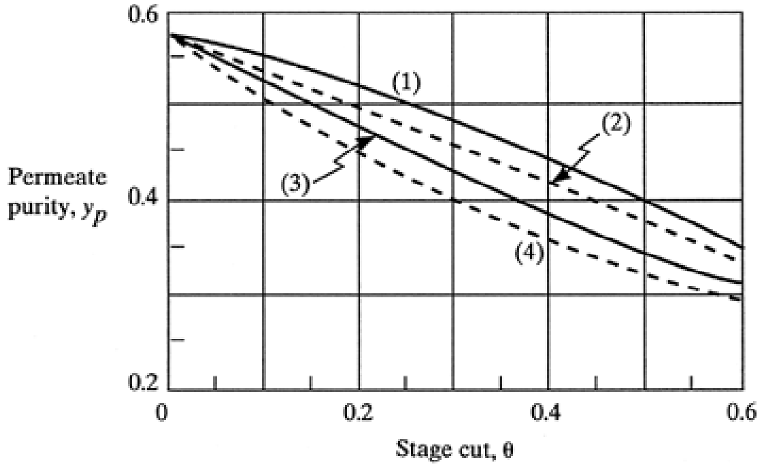

Figure 13.7-6. Effect of flow pattern in symmetric membranes. Operating conditions for air are as follows: $x_f = 0.209$, $\alpha^* = 10$, p_h/p_l *= 380 cm Hg/76 cm Hg = 5.* $P'_A = 500 \times 10^{-10}$ *cm*^{3} *(STP) · cm/s · cm*^{2} *· cm Hg. (1) countercurrent flow, (2) cross-flow, (3) cocurrent flow, (4) complete mixing (W5). [Reprinted from W. P. Walawender and S. A. Stern, Sep. Sci.,* ***7****, 553 (1972). By courtesy of Marcel Dekker, Inc.]*

The required membrane areas for the same process conditions and air feed versus stage cut were also determined (W5). The areas for all four types of flow pattern were shown to be within about 10% of each other. The countercurrent and cross-flow patterns give the lowest area required.

Effects of process flow patterns on separation in asymmetric membranes

Calculations using the mathematical models for asymmetric membranes give virtually identical performances for cocurrent and countercurrent flow (G1, P2, P6). The porous support prevents mixing of the bulk permeate concentration and the skin surface concentration y' as shown in Fig. 13.7-1b. Hence, the direction of the bulk flow permeate stream has no effect. Experimental tests using helium recovery from natural gas (P2, P6), nitrogen recovery from air (G1), and helium from nitrogen (G1) show that the experimental data and the model predictions agree quite well.

Effect of pressure drop on separations in asymmetric membranes

In hollow-fiber membranes (N1), an appreciable pressure drop can occur for flow inside long tubes or for tubes with very small inside diameters. In the shell side the pressure drop is generally very small and is neglected. Pressure drop in the tubes is always detrimental to the separation. For feed inside the tubes, the actual average feed pressure will be less than the inlet feed pressure. If the permeate flow is inside the tubes, then the actual average permeate pressure will be higher than the permeate outlet pressure. In both of these cases, the driving force for permeation is reduced and less separation occurs.

To reduce these pressure effects, where the stage cut θ is small, giving a low permeate flow rate, it is preferable to have the large feed flow rate in the shell, where the pressure drop is small. For a high stage cut, the feed should be inside the tubes, where most of the feed permeates into the shell.

Using the model equations, the pressure drop inside the tubes can be accounted for by using the Hagen-Poisseuille equation (2.10-2) for laminar flow:

Equation 2.10-2.

$$\frac{\Delta p}{(z_2 - z_1)} = \frac{32\mu v}{D^2}$$

where $z_2 - z_1$ is total length. Writing this for a differential length dz cm and a dp_h in Pascals,

Equation 13.7-37.

$$\frac{dp_h}{dz} = \frac{-32\mu v}{D^2}$$

Converting the feed flow rate L cm^3/s at T_s and p_s (STP) to the actual velocity v at T and p_h,

Equation 13.7-38.

$$\frac{dp_h}{dz} = \frac{-128\mu}{\pi D^4 N_T}\left(L\frac{T}{T_S}\frac{p_S}{p_h}\right)$$

where N_T is the number of tubes in parallel. The average viscosity μ can be approximated by using the average mole fraction of the feed and the residual outlet. The average μ is then the sum of the mole fractions of each component times the viscosity of the pure gases. The final equation is (G1, N1, P2)

Equation 13.7-39.

$$\frac{dp_h^2}{dz} = \frac{-256\mu L T p_S}{\pi D^4 N_T T_S}$$

The area A_m can be related to z by $dA_m = \pi D N_T\, dz$. This then relates dA_m to dp_h. In integrating the model equations, a constant (uniform) p_h is first assumed (G1, P2, P7). This gives the relation between y and x and A_m. Then, using the material-balance equation (13.7-18) between L and y and x, equation (13.7-39) is used to generate a new pressure profile. This process is then repeated.

DERIVATION OF FINITE-DIFFERENCE NUMERICAL METHOD FOR ASYMMETRIC MEMBRANES

Countercurrent Flow

The flow diagram for the numerical method is shown in Fig. 13.8-1. Using the method derived by McCabe et al. (M5) and taking an area ΔA_m, the mass balances on both streams can be written as

Equation 13.8-1.

$$\Delta V = L_{\text{in}} - L_{\text{out}}$$

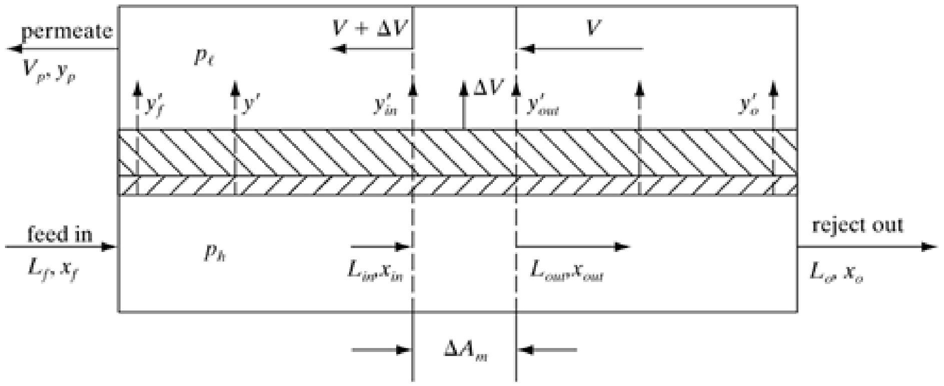

Figure 13.8-1. Flow diagram for countercurrent flow with asymmetric membrane using finite difference method.

The value of y'_{in} can be calculated from Eq. (13.7-27) using x_{in} for x and y'_{in} for y'. Also, y'_{out} can be calculated similarly from x_{out}. Then, writing a balance on A,

Equation 13.8-2.

$$\Delta V y'_{\text{av}} = L_{\text{in}} x_{\text{in}} - L_{\text{out}} x_{\text{out}}$$

where $y'_{\text{av}} = (y'_{\text{in}} + y'_{\text{out}})/2.$. Substituting L_{out} from Eq. (13.8-1) into (13.8-2),

Equation 13.8-3.

$$\Delta V = L_{\text{in}} \frac{(x_{\text{in}} - x_{\text{out}})}{(y'_{\text{av}} - x_{\text{out}})}$$

Equations (13.7-27), (13.8-2), and (13.8-3) can be solved numerically starting at the feed $x_f = x_{\text{in}}$ to determine the permeate ΔV and y'_{av} for each ΔA_m and increments of x to x_o at the outlet reject. Usually 10 or so increments of x from x_f to x_o are sufficient.

Then, to obtain the values of V and the bulk composition y as a function of x, the calculation is started at x_o. Using Equations (13.8-4) and (13.8-5), the increments of ΔV are added to get V, and y is calculated for each ΔA_m increment up to x_f at the feed inlet:

Equation 13.8-4.

$$V = \sum \Delta V$$

Equation 13.8-5.

$$y = \frac{\Sigma \, y'_{\text{av}} \, \Delta V}{V}$$

For cocurrent or parallel flow, the only difference is in calculating V. Starting at x_f inlet and using Eqs. (13.8-4) and (13.8-5), the increments of ΔV are added to get V up to x_o.

To calculate the area for countercurrent or cocurrent flow, rewriting Eq. (13.7-4),

Equation 13.8-6.

$$\frac{\Delta V y'_{\text{av}}}{\Delta A_m} = \frac{\Delta V_A}{\Delta A_m} = (P'_A/t) p_h (x - r y')_{\text{av}}$$

where $r = p_l/p_h$. The average driving force is

Equation 13.8-7.

$$(x - r y')_{\text{av}} = [(x_{\text{in}} - r y'_{\text{in}}) + (x_{\text{out}} - r y'_{\text{out}})]/2$$

Solving for ΔA_m,

Equation 13.8-8.

$$\Delta A_m = \frac{\Delta V y'_{\text{av}}}{(P'_A/t) p_h (x - r y')_{\text{av}}}$$

Starting at x_f, ΔA_m is calculated for each increment to obtain $\Sigma \, \Delta\lambda A_m$ versus x.

Short-Cut Numerical Method

Making an approximate material balance to obtain a y'_{av} or y_p for the total area from y'_f to y'_o (M5),

Equation 13.8-9.

$$y_p = y'_{\text{av}} = (y'_f + y'_o)/2$$

An overall and component material balance gives

Equation 13.8-10.

$$L_f = L_o + V_p$$

Equation 13.8-11.

$$L_f x_f = L_o x_o + V_p y_p$$

Substituting Eq. (13.8-10) into (13.8-11),

Equation 13.8-12.

$$L_f x_f = (L_f - V_p)x_o + V_p y_p$$

Equation (13.8-12) can be solved for V_p and (13.8-10) solved for L_o.

To calculate the approximate area for countercurrent or cocurrent flow, Eq. (13.8-8) is rewritten for the total area A_m:

Equation 13.8-13.

$$A_m = \frac{V_p y'_{\text{av}}}{(P'_A/t)p_h(x - ry')_{lm}}$$

where $(x - ry')_{lm}$ is the ln mean of $(x_f - ry'_f)$ and $(x_o - ry'_o)$. Since plots of x and y' versus A_m are approximately straight lines, this approximate area is within about 15% of the A_m calculated by the finite-difference method.

EXAMPLE 13.8-1. Air Separation Using an Asymmetric Membrane for Countercurrent Flow

It is desired to design a hollow-fiber asymmetric membrane for air separation to produce a residue which contains 97.0% N_2 using countercurrent flow. The dense polymer layer is in the inside of the tubes and the feed is in the tubes. Experimental values for commercial membranes give separation factors α* of O_2/N_2 between 3 and 7 (H2) with a typical value of 5.0 (*G1*). Permeance values of P'_A/t are given (H2) of 5×10^{-6} to 250×10^{-6} cm^3 (STP)/(s · cm^2 · cm Hg) with a typical value of 20×10^{-6} (G1). The typical values will be used. The feed or tube side pressure is 1034 kPa abs and the shell side or permeate is 103.4 kPa. The feed rate of air is 10.0 m^3 (STP)/h.

a. Using the finite-difference method, calculate the permeate composition, the fraction θ of feed permeated, and the residue and permeate flows. Assume negligible pressure drop in the tubes. Calculate the composition y of the permeate as a function of the residue composition x.

b. Calculate the membrane area needed.

c. Using the short-cut procedure, calculate the permeate composition, θ, flows, and membrane area.

d. Repeat (a) for cocurrent flow. Plot x, y, and y' for countercurrent and cocurrent flow versus area.

Solution: For part (a), $L_f = 10.0$ m^3 (STP)/h, $x_f = 0.209$, $x_o = 0.03$, $p_h = 1034$ kPa, $p_l = 103.4$ kPa, $P'_A/t = 20 \times 10^{-6}$ cm^3 (STP)/(s · cm^2 · cm Hg), $\alpha^* = 5.0$. Using Table 13.3-1,

$$P'_A/t = (20 \times 10^{-6})(7.501 \times 10^{-6}) = 1.500 \times 10^{-10}\,\mathrm{m^3(STP)/(s \cdot m^2 \cdot Pa)}$$

$$r = p_l/p_h = 103.4/1034 = 0.10$$

Starting at the feed inlet (Fig. 13.8-2), where $x_f = 0.209$, using an area ΔA_m, going from $x_f = x_1 = 0.209$ to $x_2 = 0.190$, and using Eq. (13.7-27) to calculate y',

Equation 13.7-27.

$$\frac{y'_1}{1 - y'_1} = \frac{\alpha^*[x_1 - (p_l/p_h)y'_1]}{(1 - x_1) - (p_l/p_h)(1 - y'_1)}$$

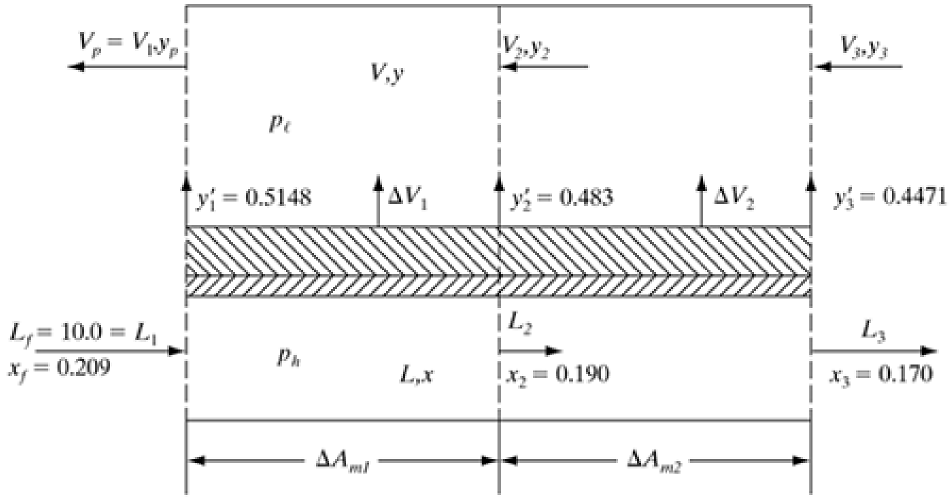

Figure 13.8-2. Finite-difference elements for countercurrent flow in Example 13.8-1.

The solution to this is given by the quadratic equation (13.4-7):

Equation 13.4-7.

$$y' = \frac{-b + \sqrt{b^2 - 4ac}}{2a}$$

where $a = 1 - \alpha^*$, $b = -1 + \alpha^* + 1/r + x/r(\alpha^* - 1)$, and $c = -\alpha^* x/r$. Substituting and solving for y'_1 where $x_1 = 0.209$,

$$x_1 = 0.209,$$

$$a = 1 - 5 = -4.0$$

$$b = -1 + 5.0 + \frac{1}{0.1} + \frac{x_1(5 - 1)}{0.1} = 14.0 + 40x_1 = 14.0 + 40(0.209) = 22.36$$

$$c = \frac{-\alpha^* x_1}{r} = \frac{-5x_1}{0.10} = -50x_1 = -50(0.209) = -10.45$$

$$y'_1 = \frac{-22.36 + [(22.36)^2 - 4(-4.0)(-10.45)]^{1/2}}{2(-4.0)} = 0.5148$$

Again, for x_2 = 0.190, y'_2 = 0.4830 is obtained from Eq. (13.7-27).

Then, $y'_{av} = (y'_1 + y'_2)/2$ = (0.5148 + 0.4830)/2 = 0.4989. Substituting into Eq. (13.8-3),

$$\Delta V_1 = \frac{L_1(x_1 - x_2)}{(y'_{av} - x_2)} = \frac{10.0(0.209 - 0.190)}{(0.4989 - 0.190)} = 0.6151 \text{ m}^3/\text{h}$$

Then by Eq. (13.8-1),

$$L_2 = L_1 - \Delta V_1 = 10.0 - 0.6151 = 9.3849 \text{ m}^3/\text{h}$$

$$y'_{av}\,\Delta V_1 = 0.4989(0.6151) = 0.3069$$

For the second increment for ΔA_{m2} in Fig. 13.8-2, solving for y'_3 with x_3 = 0.170,

$$a = -4.0, \qquad b = 14.0 + 40(10.170) = 20.8, \qquad c = -50(0.170) = -8.5$$

Using Eq. (13.4-7), y'_3 = 0.4471. Then $y'_{av} = (y'_2 + y'_3)/2$ = (0.4830 + 0.4471)/2 = 0.4651

$$\Delta V_2 = \frac{L_2(x_2 - x_3)}{(y'_{av} - x_3)} = 9.3849\frac{(0.190 - 0.170)}{(0.4651 - 0.170)} = 0.6360 \text{ m}^3/\text{h}$$

Also,

$$L_3 = L_2 - \Delta V_2 = 9.3849 - 0.6360 = 8.7489 \text{ m}^3/\text{h}$$

$$y'_{av}\,\Delta V_2 = 0.4651(0.6360) = 0.2958$$

This is continued, and for the eighth increment, x_8 = 0.07, x_9 = 0.050, y'_8 = 0.2198, y'_9 = 0.1629, y'_{av} = 0.1914, ΔV_8 = 0.7757, and L_9 = 4.7088. For the final or ninth increment, $x_{10} = x_o$ = 0.030, x_9 = 0.050, y'_9 = 0.1629, y'_{10} = 0.1014, y'_{av} = 0.1322, ΔV_9 = 0.9215, and $L_{10} = L_o$ = 3.7873 m^3/h. The permeate flow rate $V_p = L_f - L_o$ = 10.00 - 3.7873 = 6.2127 m^3/h. The stage cut θ = 6.2127/10.00 = 0.6213.

To calculate the bulk composition y as a function of x for countercurrent flow, it is necessary to start at x_o. Using Eq. (13.8-4),

$$V_9 = \sum \Delta V = V_{10} + \Delta V_9 = 0 + 0.9215 = 0.9215$$

For calculation of y_9 using Eq. (13.8-5),

$$y_9 = \frac{\sum y'_{av}\,\Delta V_9}{V_9} = \frac{0.1322(0.9215)}{0.9215} = \frac{0.1218}{0.9215} = 0.1322$$

For the eighth plus ninth increments,

$$V_8 = \sum \Delta V = V_9 + \Delta V_8 = 0.9215 + 0.7757 = 1.6972$$

$$y_8 = \frac{\sum y'_{av}\,\Delta V}{V} = \frac{0.1218 + 0.1914(0.7757)}{1.6972} = 0.1593$$

This calculation is continued up to the feed entrance. Values of *y, x,* and *y′* are given in Table 13.8-1.

Table 13.8-1. Compositions and Areas for Numerical Method in Example 13.8-1

X	*Countercurrent y*	*Cocurrent y*	*Counter and Cocurrent y′*	*ΔA, Area* (m^2)	*A, Area* (m^2)
0.209	0.3181	0.5148	0.5148	0.000	0.000
0.190	0.2983	0.4989	0.4830	3.674	3.674
0.170	0.2769	0.4817	0.4471	3.968	7.642
0.150	0.2549	0.4637	0.4084	4.117	11.759
0.130	0.2323	0.4446	0.3665	4.323	16.082
0.110	0.2090	0.4242	0.3214	4.607	20.689
0.090	0.1847	0.4021	0.2726	5.006	25.695
0.070	0.1593	0.3779	0.2198	5.592	31.287
0.050	0.1322	0.3505	0.1629	6.508	37.795
0.030	0.1014	0.3181	0.1014	8.144	**45.939**

To calculate y as a function of x for cocurrent flow, it is necessary to start at x_f. For the first increment, from Eq. (13.8-4),

$$V_1 = \sum \Delta V = 0 + \Delta V_1 = 0 + 0.6151 = 0.6151$$

$$y_1 = \frac{\sum y'_{av}\,\Delta V}{V} = \frac{0.4989(0.6151)}{0.6151} = \frac{0.3069}{0.6151} = 0.4989$$

For the second increment,

$$V = \sum \Delta V = V_1 + \Delta V_2 = 0.6151 + 0.6360 = 1.2511$$

$$y_2 = \frac{0.3069 + 0.4651(0.6360)}{1.2511} = 0.4817$$

This calculation is continued up to the outlet at x_o.

For part (b), Eq. (13.8-8) is used starting at x_f for both countercurrent and cocurrent flows. For the first increment, the flow rates in m^3/h are converted to m^3/s by multiplying by (1/3600). Also, $x_f = 0.209$, $x_2 = 0.190$, $y'_1 = 0.5148$, $y'_2 = 0.4830$, $y'_{av} = 0.4989$, $\Delta V_1 = 0.6151\ m^3/h$, and $p_h = 1034$ kPa. Calculating $x - ry'$ at points 1 and 2 and the average $(x - ry')$ from Eq. (13.8-7),

$$x_1 - ry'_1 = 0.209 - 0.10(0.5148) = 0.15752$$

$$x_2 - ry'_2 = 0.190 - 0.10(0.4830) = 0.14170$$

$$(x - ry')_{av} = (0.15752 + 0.14170)/2 = 0.1496$$

Using Eq. (13.8-8),

$$\Delta A_{m1} = \frac{(0.6151)(1/3600)(0.4989)}{(1.500 \times 10^{-10})(1034 \times 10^3)(0.1496)} = 3.674\ \text{m}^2$$

For the second increment, $x_3 = 0.170$, $y'_3 = 0.4471$, $y'_{av} = 0.4651$, and $\Delta V_2 = 0.6360$. Then,

$$x_2 - ry_2' = 0.14170$$

$$x_3 - ry_3' = 0.170 - 0.10(0.4471) = 0.12529$$

$$(x - ry')_{av} = (0.14170 + 0.12529)/2 = 0.13350$$

$$\Delta A_{m2} = \frac{(0.6360)(1/3600)(0.4651)}{(1.500 \times 10^{-10})(1034 \times 10^3)(0.13350)} = 3.968 \text{ m}^2$$

This is continued, and the results are given in Table 13.8-1. The final total area is 45.94 m^2.

For part (c), using the shortcut procedure, Eq. (13.8-9) gives the value of y_p:

$$y_p = y'_{av} = (y'_f + y'_o)/2 = (0.5148 + 0.1014)/2 = 0.3081$$

This value of 0.3081 compares to 0.3181 for the numerical method. Making a component balance in Eq. (13.8-12),

$$L_f x_f = (L_f - V_p)x_o + V_p y_p$$

$$10.0(0.209) = (10.0 - V_p)0.03 + V_p(0.3081)$$

Solving, V_p = 6.437 and L_o = (10.00 - 6.437) = 3.563. This gives a stage cut θ = 6.437/10.00 = 0.6437, as compared with 0.6213 for the numerical method. To calculate the area, the driving forces are

$$x_f - ry_f' = 0.209 - 0.10(0.5148) = 0.15752$$

$$x_o - ry_o' = 0.030 - 0.10(0.1014) = 0.01986$$

$$(x - ry')_{lm} = \frac{(0.15752 - 0.01986)}{\ln(0.15752/0.01986)} = 0.06648$$

The area from Eq. (13.8-13) is

$$A_m = \frac{6.437(1/3600)(0.3081)}{(1.500 \times 10^{-10})(1034 \times 10^3)(0.06648)} = 53.43 \text{ m}^2$$

This value of 53.43 is about 16% greater than the numerical method. A plot of these data for the numerical method is given in Fig. 13.8-3.

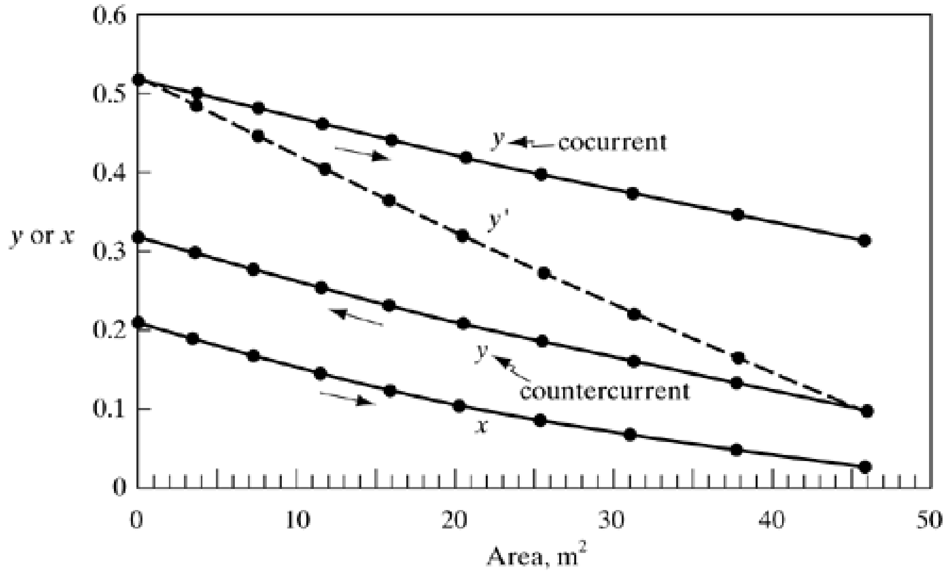

Figure 13.8-3. Plot of composition versus area for numerical method in Example 13.8-1.

Use of Spreadsheet for Finite-Difference Numerical Method

The numerical method can easily be adapted so that a spreadsheet can be used to solve the problem for asymmetric membranes. Using Excel® or other programs, basic formulas can be entered into cells.

Output data from a spreadsheet are given in Table 13.8-2 for Example 13.8-1. Input data for the calculations are briefly as follows: In cells D3-D10 known values are entered. In cell D11 the equation for $r = p_l/p_h$ is given by the formula $D$8/$D$7.

Table 13.8-2. Output from Spreadsheet for Finite-Difference Method for Example 13.8-1

Col/Row	*A*	*B*	*C*	*D*	*E*	*F*	*G*	*H*	*I*	*J*	*K*
1	Example 13.8-1										
2											
3	Input Variables:										
4	L_f (feed rate)			10	m**^{3}(STP)/hr						
5	x_f (O_2 mole fraction — feed)			0.209							
6	x_o (O_2 mole fraction — outlet)			0.03							
7	Pressure (feed), p_h			1034	kPa						

Col / Row	***A***	***B***	***C***	***D***	***E***	***F***	***G***	***H***	***I***	***J***	***K***
8	Pressure (permeate), p_l			103.4	kPa						
9	P'_A/t			1.50E-10	m**3(STP)/						
10	α*(O_2/N_2 separation factor)			5	s · m**2 · Pa						
11	$r = p_l/p_h$			0.1							
12											
13	*I*	1	2	3	4	5	6	7	8	9	10
14	*x(I)*	0.2090	0.1900	0.17	0.15	0.13	0.11	0.09	0.07	0.05	0.03
15	*A*	-4.0000	-4.0000	-4.0000	-4.0000	-4.0000	-4.0000	-4.0000	-4.0000	-4.0000	-4.0000
16	*B*	22.3600	21.6000	20.8000	20.0000	19.2000	18.4000	17.6000	16.8000	16.0000	15.2000
17	*c*	-10.4500	-9.5000	-8.5000	-7.5000	-6.5000	-5.5000	-4.5000	-3.5000	-2.5000	-1.5000
18	*y'(I)*	0.5148	0.4830	0.4471	0.4083	0.3665	0.3214	0.2726	0.2198	0.1629	0.1014
19	*y*(avg)		0.4989	0.4651	0.4277	0.3874	0.3439	0.2970	0.2462	0.1914	0.1321
20	Δ*V*		0.6151	0.6361	0.6300	0.6307	0.6401	0.6617	0.7022	0.7759	0.9219
21	*L*(I)	10.0000	9.3849	8.7487	8.1187	7.4880	6.8478	6.1861	5.4839	4.7081	3.7862
22											
23	*I*		1	2	3	4	5	6	7	8	9
24	*V*(counter)	6.2138	6.2138	5.5987	4.9626	4.3326	3.7018	3.0617	2.4000	1.6978	0.9219
25	y_{avg}*Δ*V*	1.9764	1.9764	1.6695	1.3737	1.1042	0.8599	0.6397	0.4432	0.2703	0.1218
26	*y(I)*	0.3181	0.3181	0.2982	0.2768	0.2549	0.2323	0.2089	0.1847	0.1592	0.1321
27											
28	Checks:										
29	Mass(in)	10.0000									
30	Mass(out)	10.0000									
31	$[O_2]_{in}$	2.0900									
32	$[O_2]_{out}$	2.0900									
33											
34	*I*		1	2	3	4	5	6	7	8	9
35	*V*(cocurr)		0.6151	1.2513	1.8813	2.5120	3.1522	3.8139	4.5161	5.2919	6.2138
36	y_{avg}*Δ*V*		0.3069	0.6027	0.8722	1.1166	1.3367	1.5333	1.7061	1.8546	1.9764

Col / Row	A	B	C	D	E	F	G	H	I	J	K
37	$y(I)$		0.4989	0.4817	0.4636	0.4445	0.4241	0.4020	0.3778	0.3505	0.3181
38											
39	Calculate the Areas for each increment:										
40											
41	$(x - ry')_{avg}$	0.1496	0.1335	0.1172	0.1013	0.0856	0.0703	0.0554	0.0409	0.0268	0.0099
42	$(P'_A/t)*p_h$	0.5584									
43	ΔA	3.6735	3.9690	4.1170	4.3223	4.6063	5.0061	5.5907	6.5072	8.1449	
44	Total Area	45.9370									

Row 13 is used to keep track of the indexes used in this part of the calculation. Row 14 gives the input values of x_1, x_2, and so on. In rows 15–18 the values of *a, b, c,* and y' are calculated using Eqs. (13.4-7) and (13.7-27). For example, in cell B18 the formula entered is =(-B16+SQRT(B16*B16-4*B15*B17))/2*B15). In row 19, $y'_{av} = (y'_1 + y'_2)/2$. In row 20, ΔV is calculated from Eq. (13.8-3). The formula in cell C20 is =B21*(B14-C14)/ (C19-C14) and in D20 is =C21*(C14-D14)/(D19-D14). In row 21, L is calculated from Eq. (13.8-1), where $L_2 = L_1 - \Delta V_1$ by using the formula in cell C21, which is = -(C20-B21), for C22, =-(D20-B21), and so on.

Row 23 is a new set of indexes for countercurrent flow. To calculate V in row 24 using Eq. (13.8-4), where $V = \sum \Delta V$, and starting at the outlet x_o, the formula in cell K24 is =K20, in J24, = J20+K24, and so on. For row 25, to calculate $\sum y'_{av} \Delta V$, the formula in cell K25 is =K19*K20, in J25, J19*J20+K25, and so on. For the bulk permeate composition, y is calculated in row 26 from Eq. (13.8-5), where $y = \sum y'_{av} \Delta V/V$. In cell B26, the formula is =B25/B24.

Rows 28-32 are optional and are used to check the mass balances for the inlet and outlet streams. In cell B29, the mass in is =$D$4; the mass out in B30 is =B24+K21. Similarly, cell B31 is =$D$4*$D$5 and B32 is =B24*B26+K21*K14.

For cocurrent flow, starting at x_f, Eq. (13.8-4), where $V = \sum \Delta V$, is calculated in row 35. In row 36, $\sum y'_{av} \Delta V$ is calculated using the formula in cell C36 of =19*C20, in D36, =D19*D20+C36, and so on. Then Eq. (13.8-5) is used to calculate the bulk composition y from $\sum y'_{av} \Delta V/V$ in row 37.

To calculate the areas, in row 41 $(x - ry')_{av}$ is calculated for each increment, using Eq. (13.8-7). The formula in cell B41 is =((B14-$D$11*B18) + (C14-$D$11*C18))/2. In cell B42 the conversion of V m^3/h to m^3/s and kPa to Pa is performed using = ($D$9*$D$7*1000*3600). In row 43, using Eq. (13.8-8) to calculate ΔA_m, the formula in cell B43 is C19*C20/($B$42*B41). In row 44 all of the ΔA_m values in row 43 are added to get the total A_m using =SUM(B43:J43).

Calculation of Pressure-Drop Effects on Permeation

Estimation of number of tubes and length

In order to calculate the pressure drop inside the hollow-fiber tubes, the dimensions, number of tubes, and area A_m of the membrane must be known. The following procedure can be employed.

The shortcut procedure is first used with Eqs. (13.8-9)-(13.8-13). This gives L_f, L_o, V_p, y'_{av}, and A_m. Then the average flow rate in the tubes is calculated from the equation $L_{\text{av}} = (L_f + L_o)/2$.

The number of tubes in parallel N_T must be estimated from typical laboratory or commercial data. For example, for air with a flow rate of 3 m^3/h, 3.8×10^4 fibers (N_T) are used with an ID of 95 μm, and a length ($z_2 - z_1$) of 48.26 cm. For a flow rate L_f of 10.0 m^3/hr in Example 13.8-1 and to keep a similar and reasonable velocity in the tubes, the N_T needed will be directly proportional to the inlet L_f. Then, knowing the A_m, an estimated total length ($z_2 - z_1$) of the tubes can be calculated from Eq. (13.8-14):

Equation 13.8-14.

$$A_m = \pi D N_T (z_2 - z_1)$$

Finite-difference method to include effect of pressure drop

For the finite-difference numerical method, Eq. (13.8-14) can be rewritten as

Equation 13.8-15.

$$\Delta A_m = \pi D N_T (\Delta z)$$

Also, Eq. (13.7-38) can be rewritten for a finite increment of Δz length:

Equation 13.8-16.

$$\frac{\Delta p_h}{\Delta z} = \frac{-128\mu}{\pi D^4 N_T}\left(L\frac{T}{T_S}\frac{p_S}{p_{h\,\text{av}}}\right)$$

The following steps, which may require several iterations, can be used in the finite-difference numerical method to include the effect of pressure drop in the tubes:

1. For the first increment shown in Fig. 13.8-2, a constant inlet pressure p_{h1} (p_h) is used for $p_{h\text{av}}$ to calculate y'_1 and y'_2, ΔV_1, L_2, and ΔA_{m1} from Eqs. (13.7-27), (13.8-1), (13.8-3), (13.8-7), and (13.8-8).
2. The value of N_T is obtained from typical data as discussed above in Subsection 1. Using Eq. (13.8-15), the incremental length Δz is obtained.
3. Using $L_{\text{av}} = (L_1 + L_2)/2$ and the inlet p_{h1} for $p_{h\,\text{av}}$, the Δp_h for the first increment is calculated from Eq. (13.8-16).
4. For the second iteration, the new $p_{h\,\text{av}}$ to use is calculated from $p_{h\,\text{av}} = p_{h1} - \Delta p_h/2$. A new value of the outlet $p_{h2} = p_{h1} - \Delta p_h$ is used to recalculate a new y'_2 from Eq. (13.7-27). The value of y'_1 remains the same. Then by repeating steps 1 through 4, a new value of Δp_h is obtained. Usually only three or so iterations are needed to obtain a constant value of Δp_h, $p_{h\text{av}}$, and ΔA_{m1}. Using a spreadsheet as in Ex. 13.8-1, this procedure can be repeated for each finite section.

Determination of effect of pressure drop using shortcut method

The values of L_{av}, N_T, A_m, and overall length ($z_2 - z_1$) are obtained from the shortcut calculation in Subsection 1 above. The shortcut value of the overall pressure drop ($p_h - p_{ho}$) can be obtained from Eq. (13.8-16) using p_h at the inlet as $p_{h\ av}$ and the overall length ($z_2 - z_1$). Then for a second and final iteration, the new and corrected pressures $p_{h\ av} = p_h - \Delta p_h/2$ and $p_{ho} = p_h - \Delta p_h$ are used in Eqs. (13.7-27) and (13.8-9)-(13.8-13) to recalculate y'_o, y'_{av}, V_p, and A_m again. This recalculated A_m will include an approximate effect of pressure drop in the tubes.

REVERSE-OSMOSIS MEMBRANE PROCESSES

Introduction

Introduction

To be useful for separation of different species, a membrane must allow passage of certain molecules and exclude or greatly restrict passage of others. In osmosis, a spontaneous transport of solvent occurs from a dilute solute or salt solution to a concentrated solute or salt solution across a semipermeable membrane which allows passage of the solvent but impedes passage of the salt solutes. In Fig. 13.9-1a, the solvent water normally flows through the semipermeable membrane to the salt solution. The levels of both liquids are the same as shown. The solvent flow can be reduced by exerting a pressure on the salt-solution side and membrane, as shown in Fig. 13.9-1b, until at a certain pressure, called the osmotic pressure π of the salt solution, equilibrium is reached and the amount of the solvent passing in opposite directions is equal. The chemical potentials of the solvent on both sides of the membrane are equal. The properties of the solution determine only the value of the osmotic pressure, not the membrane, provided that it is truly semipermeable. To reverse the flow of the water so that it flows from the salt solution to the fresh solvent, as in Fig. 13.9-1c, the pressure is increased above the osmotic pressure on the solution side.

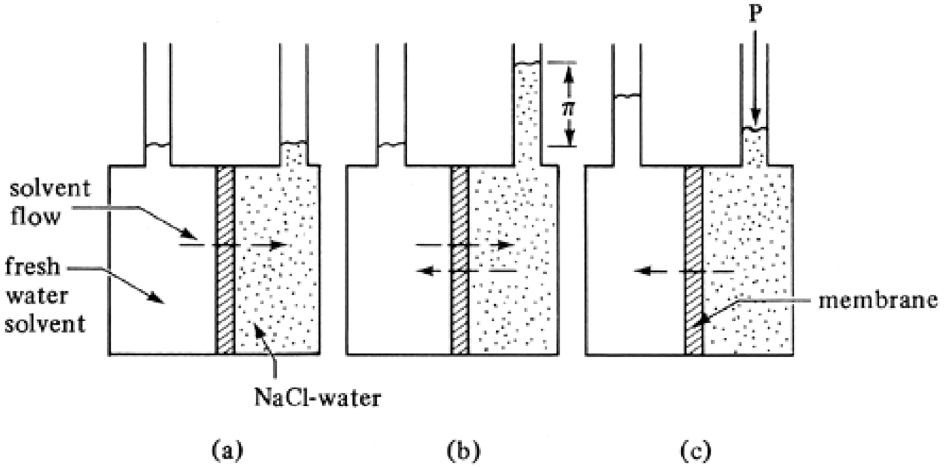

Figure 13.9-1. Osmosis and reverse osmosis: (a) osmosis, (b) osmotic equilibrium, (c) reverse osmosis.

This phenomenon, called *reverse osmosis,* is used in a number of processes. An important commercial use is in the desalination of seawater or brackish water to produce fresh water. Unlike distillation and freezing processes used to remove solvents, reverse osmosis can operate at ambient temperature without phase change. This process is quite useful for the processing of thermally and chemically unstable products. Applications include concentration of fruit juices and milk, recovery of protein and sugar from cheese whey, and concentration of enzymes.

Osmotic pressure of solutions

Experimental data show that the osmotic pressure π of a solution is proportional to the concentration of the solute and temperature T. Van't Hoff originally showed that the relationship is similar to that for pressure of an ideal gas. For example, for dilute water solutions,

Equation 13.9-1.

$$\pi = \frac{n}{V_m} RT$$

where n is the number of kg mol of solute, V_m the volume of pure solvent water in m^3 associated with n kg mol of solute, R the gas law constant 82.057×10^{-3} $m^3 \cdot$ atm/kg mol $\cdot$ K, and T is temperature in K. If a solute exists as two or more ions in solution, n represents the total number of ions. For more concentrated solutions, Eq. (13.9-1) is modified using the osmotic coefficient ϕ, which is the ratio of the actual osmotic pressure π to the ideal π calculated from the equation. For very dilute solutions, ϕ has a value of unity and usually decreases as concentration increases. In Table 13.9-1 some experimental values of π are given for NaCl solutions, sucrose solutions, and seawater solutions (S3, S5).

Table 13.9-1. Osmotic Pressure of Various Aqueous Solutions at 25°C (P1, S3, S5)

Sodium Chloride Solutions			*Sea Salt Solutions*		*Sucrose Solutions*	
$\frac{g\,mol\,NaCl}{kg\,H_2O}$	*Density (kg/ m^3)*	*Osmotic Pressure (atm)*	*Wt % Salts*	*Osmotic Pressure (atm)*	*Solute Mol. Frac. × 10^3*	*Osmotic Pressure (atm)*
0	997.0	0	0	0	0	0
0.01	997.4	0.47	1.00	7.10	1.798	2.48
0.10	1001.1	4.56	3.45*	25.02	5.375	7.48
0.50	1017.2	22.55	7.50	58.43	10.69	15.31
1.00	1036.2	45.80	10.00	82.12	17.70	26.33
2.00	1072.3	96.2				

*Value for standard seawater.

EXAMPLE 13.9-1. Calculation of Osmotic Pressure of Salt Solution

Calculate the osmotic pressure of a solution containing 0.10 g mol NaCl/1000 g H_2O at 25°C.

Solution: From Table A.2-3, the density of water = 997.0 kg/m^3. Then, $n = 2 \times 0.10 \times 10^{-3} = 2.00 \times 10^{-4}$ kg mol (NaCl gives two ions). Also, the volume of the pure solvent water V_m = 1.00 kg/(997.0 kg/m^3). Substituting into Eq. (13.9-1),

$$\pi = \frac{n}{V_m} RT = \frac{2.00 \times 10^{-4}(82.057 \times 10^{-3})(298.15)}{1.000/997.0} = 4.88 \text{ atm}$$

This compares with the experimental value in Table 13.9-1 of 4.56 atm.

Types of membranes for reverse osmosis

One of the more important membranes for reverse-osmosis desalination and many other reverse-osmosis processes is the cellulose acetate membrane. The asymmetric membrane is made as a composite film in which a thin, dense layer about 0.1–10 μm thick of extremely fine pores is supported upon a much thicker (50–125 μm) layer of microporous sponge with little resistance to permeation. The thin, dense layer has the ability to block the passage of quite small solute molecules. In desalination the membrane rejects the salt solute and allows the solvent water to pass through.

Solutes which are most effectively excluded by the cellulose acetate membrane are the salts NaCl, NaBr, $CaCl_2$, and Na_2SO_4; sucrose; and tetralkyl ammonium salts. The main limitations of the cellulose acetate membrane are that for the most part it can only be used in aqueous solutions and that it must be used below about 60°C.

Another important membrane useful for seawater, wastewater, nickel-plating rinse solutions, and other solutes is the synthetic aromatic polyamide membrane "Permasep," made in the form of very fine, hollow fibers (L1, P3). When used industrially this type of membrane withstands continued operation at pH values of 10 to 11 (S4). Many other anisotropic membranes have also been synthesized from synthetic polymers, some of which can be used in organic solvents, at higher temperatures, and at high or low pH (M2, Rl).

Flux Equations for Reverse Osmosis

Basic models for membrane processes

There are two basic types of mass-transport mechanisms which can take place in membranes. In the first basic type, using tight membranes, which are capable of retaining solutes of about 10 Å in size or less, diffusion-type transport mainly occurs. Both the solute and the solvent migrate by molecular or Fickian diffusion in the polymer, driven by concentration gradients set up in the membrane by the applied pressure difference. In the second basic type, using loose, microporous membranes which retain particles larger than 10 Å, a sieve-type mechanism occurs, where the solvent moves through the micropores in essentially viscous flow and the solute molecules small enough to pass through the pores are carried by convection with the solvent. For details of this second type of mechanism, see (M2, W1).

Diffusion-type model

For diffusion-type membranes, the steady-state equations governing the transport of solvent and solute are to a first approximation as follows (M2, M3). For the diffusion of the solvent through the membrane, as shown in Fig. 13.9-2,

Equation 13.9-2.

$$N_w = \frac{P_w}{L_m}(\Delta P - \Delta \pi) = A_w(\Delta P - \Delta \pi)$$

Equation 13.9-3.

$$A_w = \frac{P_w}{L_m}$$

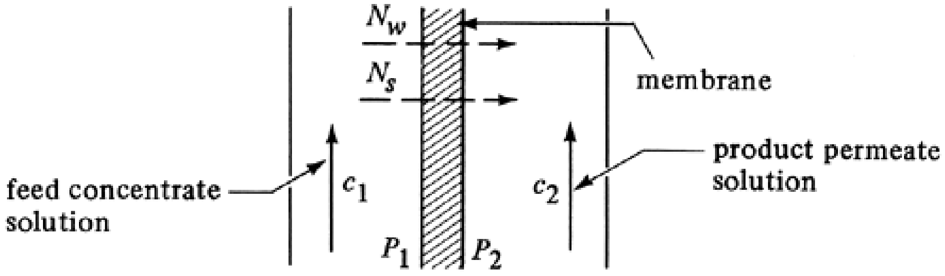

Figure 13.9-2. Concentrations and fluxes in reverse-osmosis process.

where N_w is the solvent (water) flux in kg/s · m^2; P_w the solvent membrane permeability, kg solvent/s · m · atm; L_m the membrane thickness, m; A_w the solvent permeability constant, kg solvent/s · m^2 · atm; $\Delta P = P_1 - P_2$ (hydrostatic pressure difference with P_1 pressure exerted on feed and P_2 on product solution), atm; and $\Delta\pi = \pi_1 - \pi_2$ (osmotic pressure of feed solution — osmotic pressure of product solution), atm. Note that subscript 1 is the feed or upstream side of the membrane and 2 the product or downstream side of the membrane.

For the diffusion of the solute through the membrane, an approximation for the flux of the solute is (Cl, Ml)

Equation 13.9-4.

$$N_s = \frac{D_s K_s}{L_m}(c_1 - c_2) = A_s(c_1 - c_2)$$

Equation 13.9-5.

$$A_s = \frac{D_s K_s}{L_m}$$

where N_s is the solute (salt) flux in kg solute/s · m^2; D_s the diffusivity of solute in membrane, m^2/s; $K_s = c_m/c$ (distribution coefficient), concentration of solute in membrane/concentration of solute in solution; A_s is the solute permeability constant, m/s; c_1 the solute concentration in upstream or feed (concentrate) solution, kg solute/m^3; and c_2 the solute concentration in downstream or product (permeate) solution, kg solute/m^3. The distribution coefficient K_s is approximately constant over the membrane.

Making a material balance at steady state for the solute, the solute diffusing through the membrane must equal the amount of solute leaving in the downstream or product (permeate) solution:

Equation 13.9-6.

$$N_s = \frac{N_w c_2}{c_{w2}}$$

where c_{w2} is the concentration of solvent in stream 2 (permeate), kg solvent/m^3. If the stream 2 is dilute in solute, c_{w2} is approximately the density of the solvent. In reverse osmosis, the solute rejection R is defined as the ratio concentration difference across the membrane divided by the bulk concentration on the feed or concentrate side (fraction of solute remaining in the feed stream):

Equation 13.9-7.

$$R = \frac{c_1 - c_2}{c_1} = 1 - \frac{c_2}{c_1}$$

This can be related to the flux equations as follows, by first substituting Eqs. (13.9-2) and (13.9-4) into (13.9-6) to eliminate N_w and N_s in Eq. (13.9-6). Then, solving for c_2/c_1 and substituting this result into Eq. (13.9-7),

Equation 13.9-8.

$$R = \frac{B(\Delta P - \Delta\pi)}{1 + B(\Delta P - \Delta\pi)}$$

Equation 13.9-9.

$$B = \frac{P_w}{D_s K_s c_{w2}} = \frac{A_w}{A_s c_{w2}}$$

where B is in atm^{-1}. Note that B is composed of the various physical properties P_w, D_s, and K_s of the membrane and must be determined experimentally for each membrane. Usually it is the product D_sK_s that is determined, not the values of D_s and K_s separately. Also, many of the data reported in the literature give values of (P_w/L_m) or A_w in kg solvent/s · m^2 · atm and (D_sK_s/L_m) or A_s in m/s and not separate values of L_m, P_w, and so on.

EXAMPLE 13.9-2. Experimental Determination of Membrane Permeability

Experiments at 25°C were performed to determine the permeabilities of a cellulose acetate membrane (A1, W1). The laboratory test section shown in Fig. 13.9-3 has membrane area $A = 2.00 \times 10^{-3}$ m^2. The inlet feed solution concentration of NaCl is $c_1 = 10.0$ kg NaCl/m^3 solution (10.0 g NaCl/L, $\rho_1 = 1004$ kg solution/m^3). The water recovery is assumed low so that the concentration c_1 in the entering feed solution flowing past the membrane and the concentration of the exit feed solution are essentially equal. The product solution contains $c_2 = 0.39$ kg NaCl/m^3 solution ($\rho_2 = 997$ kg solution/m^3) and its measured flow rate is 1.92×10^{-8} m^3 solution/s. A pressure differential of 5514 kPa (54.42 atm) is used. Calculate the permeability constants of the membrane and the solute rejection R.

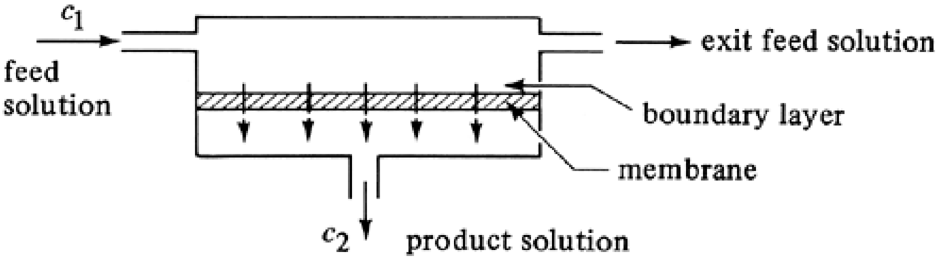

Figure 13.9-3. Process flow diagram of experimental reverse-osmosis laboratory unit.

***Solution*:** Since c_2 is very low (dilute solution), the value of c_{w2} can be assumed as the density of water (Table 13.9-1), or $c_{w2} = 997$ kg solvent/m^3. To convert the product flow rate to water flux, N_w, using an area of 2.00×10^{-3} m^2,

$$N_w = (1.92 \times 10^{-8}\ \text{m}^3/\text{s})(997\ \text{kg solvent/m}^3)(1/2.00 \times 10^{-3}\ \text{m}^2)$$
$$= 9.57 \times 10^{-3}\ \text{kg solvent/s} \cdot \text{m}^2$$

Substituting into Eq. (13.9-6),

$$N_s = \frac{N_w c_2}{c_{w2}} = \frac{(9.57 \times 10^{-3})(0.39)}{997}$$
$$= 3.744 \times 10^{-6}\ \text{kg solute NaCl/s} \cdot \text{m}^2$$

To determine the osmotic pressures from Table 13.9-1, the concentrations are converted as follows. For c_1, 10 kg NaCl is in 1004 kg solution/m^3 ($\rho_1 = 1004$). Then, 1004 - 10 = 994 kg H_2O in 1 m^3 solution. Hence, in the feed solution, where the molecular weight of NaCl = 58.45, (10.00 × 1000)/ (994 × 58.45) = 0.1721 g mol NaCl/kg H_2O. From Table 13.9-1, $\pi_1 = 7.80$ atm by linear interpolation. Substituting into Eq. (13.9-1), the predicted $\pi_1 = 8.39$ atm, which is higher than the experimental value. For the product solution, 997 - 0.39 = 996.6 kg H_2O. Hence, (0.39 × 1000)/(996.6 × 58.45) = 0.00670 g mol NaCl/kg H_2O. From Table 13.9-1, $\pi_2 = 0.32$ atm. Then, $\Delta\pi = \pi_1 - \pi_2 = 7.80 - 0.32 = 7.48$ atm and $\Delta P = 54.42$ atm.

Substituting into Eq. (13.9-2),

$$N_w = 9.57 \times 10^{-3} = \frac{P_w}{L_m}(\Delta P - \Delta\pi) = \frac{P_w}{L_m}(54.42 - 7.48)$$

Solving, $(P_w/L_m) = A_w = 2.039 \times 10^{-4}$ kg solvent/s · m^2 · atm. Substituting into Eq. (13.9-4),

$$N_s = 3.744 \times 10^{-6} = \frac{D_s K_s}{L_m}(c_1 - c_2) = \frac{D_s K_s}{L_m}(10.00 - 0.39)$$

Solving, $(D_s K_s/L_m) = A_s = 3.896 \times 10^{-7}$ m/s.

To calculate the solute rejection R by substituting into Eq. (13.9-7),

$$R = \frac{c_1 - c_2}{c_1} = \frac{10.00 - 0.39}{10.00} = 0.961$$

Also, substituting into Eq. (13.9-9) and then Eq. (13.9-8),

$$B = \frac{P_w/L_m}{(D_s K_s/L_m)c_{w2}} = \frac{2.039 \times 10^{-4}}{(3.896 \times 10^{-7})997} = 0.5249 \text{ atm}^{-1}$$

$$R = \frac{B(\Delta P - \Delta\pi)}{1 + B(\Delta P - \Delta\pi)} = \frac{0.5249(54.42 - 7.48)}{1 + 0.5249(54.42 - 7.48)} = 0.961$$

APPLICATIONS, EQUIPMENT, AND MODELS FOR REVERSE OSMOSIS

Effects of Operating Variables

In many commercial units, operating pressures in reverse osmosis range from about 1035 up to 10350 kPa (150 up to 1500 psi). Comparison of Eq. (13.9-2) for solvent flux with Eq. (13.9-4) for solute flux shows that the solvent flux N_w depends only on the net pressure difference, while the solute flux N_s depends only on the concentration difference. Hence, as the feed pressure is increased, solvent or water flow through the membrane increases and the solute flow remains approximately constant, giving lower solute concentration in the product solution.

At a constant applied pressure, increasing the feed solute concentration increases the product solute concentration. This is caused by the increase in the feed osmotic pressure, since as more solvent is extracted from the feed solution (as water recovery increases), the solute concentration becomes higher and the water flux decreases. Also, the amount of solute present in the product solution increases because of the higher feed concentration.

If a reverse-osmosis unit has a large membrane area (as in a commercial unit), and the path between the feed inlet and outlet is long, the outlet feed concentration can be considerably higher than the inlet feed c_1. Then the salt flux will be greater at the outlet feed as compared to the inlet (K2). Many manufacturers use the feed solute or salt concentration average between inlet and outlet to calculate the solute or salt rejection R in Eq. (13.9-7).

EXAMPLE 13.10-1. Prediction of Performance in a Reverse-Osmosis Unit

A reverse-osmosis membrane to be used at 25°C for a NaCl feed solution containing 2.5 g NaCl/L (2.5 kg NaCl/m^3, ρ = 999 kg/m^3) has a water permeability constant A_w = 4.81 × 10^{-4} kg/s · m^2 · atm and a solute (NaCl) permeability constant A_s = 4.42 × 10^{-7} m/s (A1). Calculate the water flux and solute flux through the membrane using ΔP = 27.20 atm and the solute rejection R. Also calculate c_2 of the product solution.

Solution: In the feed solution, c_1 = 2.5 kg NaCl/m^3 and ρ_1 = 999 kg solution/m^3. Hence, for the feed, 999 - 2.5 = 996.5 kg H_2O in 1.0 m^3 solution: also for the feed, (2.50 × 1000)/(996.5 × 58.45) = 0.04292 g mol NaCl/kg H_2O. From Table 13.9-1, π_1 = 1.97 atm. Since the product solution c_2 is unknown, a value of c_2 = 0.1 kg NaCl/m^3 will be assumed. Also, since this is quite dilute, ρ_2 = 997 kg solution/m^3 and C_{w2} = 997 kg solvent/m^3. Then for the product solution, (0.10 × 1000)/(996.9 × 58.45) = 0.00172 g mol NaCl/kg H_2O and π_2 = 0.08 atm. Also, $\Delta\pi = \pi_1 - \pi_2$ = 1.97 - 0.08 = 1.89 atm.

Substituting into Eq. (13.9-2),

$$N_w = A_w(\Delta P - \Delta\pi) = 4.81 \times 10^{-4}(27.20 - 1.89)$$

$$= 1.217 \times 10^{-2}\ \text{kg H}_2\text{O/s} \cdot \text{m}^2$$

For calculation of R, substituting first into Eq. (13.9-9),

$$B = \frac{A_w}{A_s c_{w2}} = \frac{4.81 \times 10^{-4}}{4.42 \times 10^{-7} \times 997} = 1.092\ \text{atm}^{-1}$$

Next, substituting into Eq. (13.9-8),

$$R = \frac{B(\Delta P - \Delta\pi)}{1 + B(\Delta P - \Delta\pi)} = \frac{1.092(27.20 - 1.89)}{1 + 1.092(27.20 - 1.89)} = 0.965$$

Using this value of R in Eq. (13.9-7),

$$R = 0.965 = \frac{c_1 - c_2}{c_1} = \frac{2.50 - c_2}{2.50}$$

Solving, c_2 = 0.0875 kg NaCl/m^3 for the product solution. This is close enough to the assumed value of c_2 = 0.10 that π_2 will not change significantly on a second trial. Hence, the final value of c_2 is 0.0875 kg NaCl/m^3 (0.0875 g NaCl/L).

Substituting into Eq. (13.9-4),

$$N_s = A_s(c_1 - c_2) = 4.42 \times 10^{-7}(2.50 - 0.0875)$$

$$= 1.066 \times 10^{-6}\ \text{kg NaCl/s} \cdot \text{m}^2$$

Concentration Polarization in Reverse-Osmosis Diffusion Model

In desalination, localized concentrations of solute build up at the point where the solvent leaves the solution and enters the membrane. The solute accumulates in a relatively stable boundary layer (Fig. 13.9-3) next to the membrane. Concentration polarization, β, is defined as the ratio of the salt concentration at the membrane surface to the salt concentration in the bulk feed stream c_1. Concentration polarization causes the water flux to decrease, since the osmotic pressure π_1 increases as the boundary layer concentration increases and the overall driving force ($\Delta P - \Delta\pi$) decreases. Also, the solute flux increases, since the solute concentration increases at the boundary. Hence, often the ΔP must be increased to compensate, which results in higher power costs (K2).

The effect of the concentration polarization β can be included approximately by modifying the value of $\Delta\pi$ in Eqs. (13.9-2) and (13.9-8) as follows (P6):

Equation 13.10-1.

$$\Delta\pi = \beta\pi_1 - \pi_2$$

It is assumed that the osmotic pressure π_1 is directly proportional to the concentration, which is approximately correct. Also, Eq. (13.9-4) can be modified as

Equation 13.10-2.

$$N_s = A_s(\beta c_1 - c_2)$$

The usual concentration polarization ratio (K3) is 1.2 to 2.0, that is, the concentration in the boundary layer is 1.2-2.0 times c_1 in the bulk feed solution. This ratio is often difficult to predict. In desalination of seawater, using values of about 1000 psia = ΔP, π_1 can be large. Increasing this π_1 by a factor of 1.2-2.0 can appreciably reduce the solvent flux. For brackish waters containing 2–10 g/L and using ΔP values of 17–55 atm abs, the value of π_1 is low and concentration polarization is not important.

The boundary layer can be reduced by increasing the turbulence by using higher feed-solution velocities. However, this extra flow results in a smaller ratio of product solution to feed. Also, screens can be put in the path to induce turbulence. Equations for predicting the mass-transfer coefficient to the surface and, hence, the concentration polarization, are given for specific geometries such as flow past plates, inside tubes, outside tubes, and so on (H2, N1). Then equations for the flux of water can be used with these mass-transfer coefficients in a manner similar to that for ultrafiltration given in Section 13.11.

Permeability Constants for Reverse-Osmosis Membranes

Permeability constants for membranes must be determined experimentally for the particular type of membrane to be used. For cellulose acetate membranes, typical water permeability constants A_w range from about 1×10^{-4} to 5×10^{-4} kg solvent/s · m^2 · atm (A1, M3, W1). Values for other types of membranes can differ widely. Generally, the water permeability constant for a particular membrane does not depend upon the solute present. For the solute permeability constants A_S of cellulose acetate membranes, some relative typical values are as follows, assuming a value of $A_s = 4 \times 10^{-7}$ m/s for NaCl: 1.6×10^{-7} m/s ($BaCl_2$), 2.2×10^{-7} ($MgCl_2$), 2.4×10^{-7} ($CaCl_2$), 4.0×10^{-7} (Na_2SO_4), 6.0×10^{-7} (KC1), 6.0×10^{-7} (NH_4C1) (A1).

Types of Equipment for Reverse Osmosis

The equipment for reverse osmosis is quite similar to that for gas permeation membrane processes described in Section 13.3C. In the plate-and-frame-type unit, thin plastic support plates with thin grooves are covered on both sides with membranes as in a filter press. Pressurized feed solution flows between the closely spaced membranes (L1*)*. Solvent permeates through the membrane and flows in the grooves to an outlet. In the tubular-type unit, membranes in the form of tubes are inserted inside porous-tube casings, which serve as a pressure vessel. These tubes are then arranged in bundles like *a* heat exchanger.

In the spiral-wound type, a planar membrane is used and a flat, porous support material is sandwiched between the membranes. Then the membranes, support, and a mesh feed-side spacer are wrapped in a spiral around a tube. In the hollow-fiber type, fibers of 100–200 μm diameter with walls about 25 μm thick are arranged in a bundle similar to a heat exchanger (L1, R1).

Complete-Mixing Model for Reverse Osmosis

The process flow diagram for the complete-mixing model is shown in Fig. 13.10-1. The model is a simplified one for use with low concentrations of salt of about 1% or so, such as occur in brackish waters. Also, a relatively low recovery of solvent occurs and the effects of concentration polarization are small. Since the concentration of the permeate is very low, the permeate side acts as though it were completely mixed.

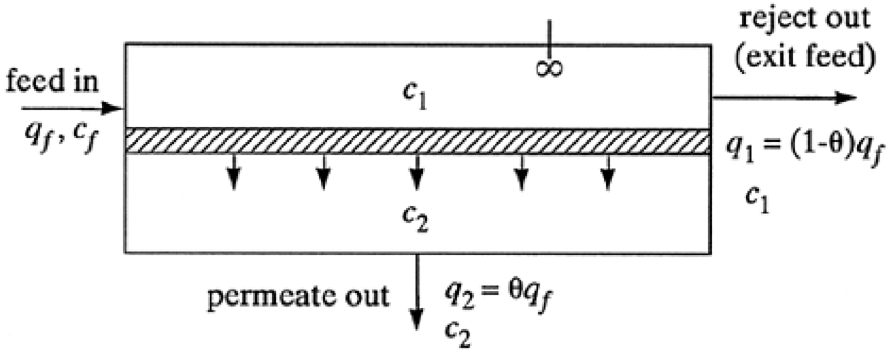

Figure 13.10-1. Process flow for complete-mixing model for reverse osmosis.

For the overall material balance for dilute solutions,

Equation 13.10-3.

$$q_f = q_1 + q_2$$

where q_f is volumetric flow rate of feed, m^3/s; q_2 is flow rate of permeate, m^3/s; and q_1 is flow rate of residue or exit, m^3/s. Making a solute balance,

Equation 13.10-4.

$$c_f q_f = c_1 q_1 + c_2 q_2$$

Defining the cut or fraction of solvent recovered as $\theta = q_2/q_f$, Eq. (13.10-4) becomes

Equation 13.10-5.

$$c_f = (1 - \theta)c_1 + \theta c_2$$

The equations previously derived for the fluxes and rejection are useful in this case and are as follows:

Equation 13.9-2.

$$N_w = A_2(\Delta P - \Delta\pi)$$

Equation 13.9-4.

$$N_s = A_s(c_1 - c_2)$$

Equation 13.9-7.

$$R = \frac{c_1 - c_2}{c_1}$$

Equation 13.9-8.

$$R = \frac{B(\Delta P - \Delta \pi)}{1 + B(\Delta P - \Delta \pi)}$$

When the cut or fraction recovered, θ, is specified, the solution is trial and error. Since the permeate and reject concentrations c_1 and c_2 are unknown, a value of c_2 is assumed. Then c_1 is calculated from Eq. (13.10-5). Next, N_w is obtained from Eq. (13.9-2) and c_2 from Eqs. (13.9-7) and (13.9-8). If the calculated value of c_2 does not equal the assumed value, the procedure is repeated.

When concentration-polarization effects are present, an estimated value of β can be used to make an approximate correction for these effects. This is used in Eq. (13.10-1) to obtain a value of $\Delta\pi$ for use in Eqs. (13.9-2) and (13.9-8). Also, Eq. (13.10-2) will replace Eq. (13.9-4). A more detailed analysis of this complete mixing model is given by others (H1, K1), in which the mass-transfer coefficient in the concentration-polarization boundary layer is used.

The cross-flow model for reverse osmosis is similar to that for gas separation by membranes which was discussed in Section 13.6. Because of the small solute concentration, the permeate side acts as if completely mixed. Hence, even if the module is designed for countercurrent or cocurrent flow, the cross-flow model is valid. This is discussed in detail elsewhere (H1).

ULTRAFILTRATION MEMBRANE PROCESSES

Introduction

Ultrafiltration is a membrane process that is quite similar to reverse osmosis. It is a pressure-driven process where the solvent and, when present, small solute molecules pass through the membrane and are collected as a permeate. Larger solute molecules do not pass through the membrane and are recovered in a concentrated solution. The solutes or molecules to be separated generally have molecular weights greater than 500 and up to 1 000 000 or more, such as macromolecules of proteins, polymers, and starches as well as colloidal dispersions of clays, latex particles, and microorganisms.

Unlike reverse osmosis, ultrafiltration membranes are too porous to be used for desalting. The rejection *R,* often called retention, is also given by Eq. (13.9-7), which is defined for reverse osmosis. Ultrafiltration is also used to separate a mixture of different-molecular-weight proteins. The molecular-weight cut-off of the membrane is defined as the molecular weight of globular proteins, which are 90% retained by the membrane. A rule of thumb is that the molecular mass must differ by a factor of 10 for a good separation (P7).

Ultrafiltration is used in many different processes at the present time. Some of these are separation of oil-water emulsions, concentration of latex particles, processing of blood and plasma, fractionation or separation of proteins, recovery of whey proteins in cheese manufacturing, removal of bacteria and other particles to sterilize wine, and clarification of fruit juices.

Membranes for ultrafiltration are in general similar to those for reverse osmosis and are commonly asymmetric and more porous. The membrane consists of a very thin, dense skin supported by a relatively porous layer for strength. Membranes are made from aromatic polyamides, cellulose acetate, cellulose nitrate, polycarbonate, polyimides, polysulfone, and so forth (M2, P6, **R1**).

Types of Equipment for Ultrafiltration

The equipment for ultrafiltration is similar to that used for reverse osmosis and gas separation processes, described in Sections 13.3C and **13.10D**. The tubular-type unit is less prone to fouling and more easily cleaned than any of the other three types; however, this type is relatively costly.

Flat sheet membranes in a plate-and-frame unit offer the greatest versatility but at the highest capital cost (P6). Membranes can easily be cleaned or replaced by disassembly of the unit. Spiral-wound modules provide relatively low costs per unit membrane area. These units are more prone to fouling than tubular units but are more resistant to fouling than hollow-fiber units. Hollow-fiber modules are the least resistant to fouling as compared to the other three types. However, the hollow-fiber configuration has the highest ratio of membrane area per unit volume.

Cross-flow filtration is the most common type of model used (P7). Spiral-wound flat sheets are used most of all, followed by hollow-fiber units. Batch processes are also quite common. Stirred tanks with a membrane are used which approximate cross-flow operation (**R1).**

Flux Equations for Ultrafiltration

The flux equation for diffusion of solvent through the membrane is the same as Eq. (13.9-2) for reverse osmosis:

Equation 13.9-2.

$$N_w = A_w(\Delta P - \Delta \pi)$$

In ultrafiltration the membrane does not allow passage of the solute, which is generally a macromolecule. The concentration in moles/liter of the large solute molecules is usually small. Hence, the osmotic pressure is very low and can be neglected. Then Eq. (13.9-2) becomes

Equation 13.11-1.

$$N_w = A_w(\Delta P)$$

Ultrafiltration units operate at about 5–100 psi pressure drop, compared to 400-2000 for reverse osmosis. For low-pressure drops of, say, 5–10 psi and dilute solutions of up to 1 wt % or so, Eq. (13.11-1) predicts the performance reasonably well for well-stirred systems.

Since the solute is rejected by the membrane, it accumulates and starts to build up at the surface of the membrane. As pressure drop is increased and/or concentration of the solute is increased, concentration polarization occurs, which is much more severe than in reverse osmosis. This is shown in Fig. 13.11-1a, where c_1 is the concentration of the solute in the bulk solution, kg solute/m^3, c_s is the concentration of the solute at the surface of the membrane, and c_p is the concentration in the permeate.

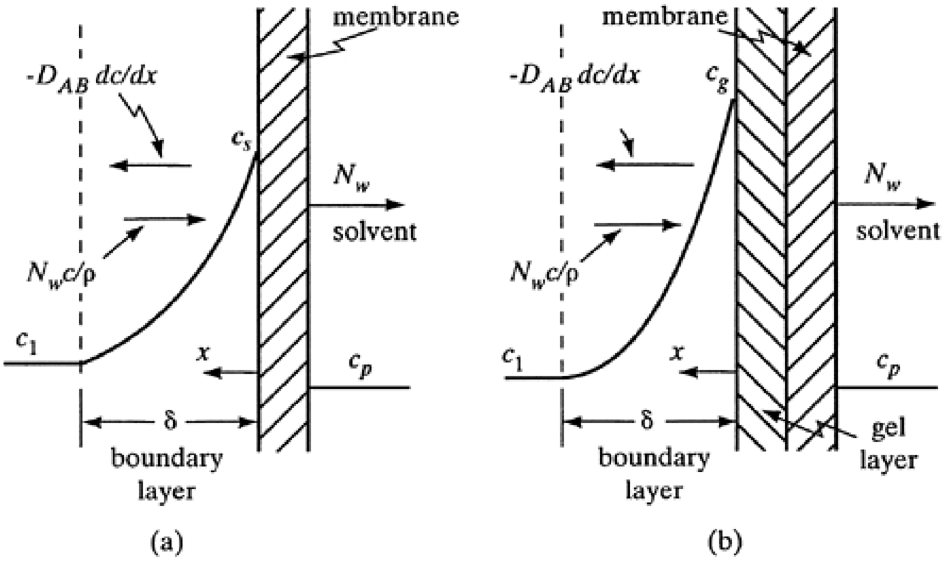

Figure 13.11-1. Concentration polarization in ultrafiltration: (a) concentration profile before gel formation, (b) concentration profile with a gel layer formed at membrane surface.

As the pressure drop increases, this increases the solvent flux N_w to and through the membrane. This results in a higher convective transport of the solute to the membrane, that is, the solvent carries with it more solute. The concentration c_s increases and gives a larger back molecular diffusion of solute from the membrane to the bulk solution. At steady state the convective flux equals the diffusion flux:

Equation 13.11-2.

$$\frac{N_w c}{\rho} = -D_{AB}\frac{dc}{dx}$$

where N_wc/ρ = [kg solvent/(s · m^2)](kg solute/m^3)/(kg solvent/m^3) = kg solute/s · m^2; D_{AB} is diffusivity of solute in solvent, m^2/s; and x is distance, m. Integrating this equation between the limits of $x = 0$ and $c = c_s$ and $x = \delta$ and $c = c_1$,

Equation 13.11-3.

$$\frac{N_w}{\rho} = \left(\frac{D_{Ab}}{\delta}\right)\ln\left(\frac{c_s - c_p}{c_1 - c_p}\right) = k_c \ln\left(\frac{c_s - c_p}{c_1 - c_p}\right)$$

where k_c is the mass-transfer coefficient, m/s. Further increases in pressure drop increase the value of c_s to a limiting concentration, at which the accumulated solute forms a semisolid gel where $c_s = c_g$, as shown in Fig. 13.11-1b. For the usual case of almost-complete solute retention (P7), $c_p = 0$ and Eq. (13.11-3) becomes

Equation 13.11-4.

$$\frac{N_w}{\rho} = k_c \ln(c_s/c_1)$$

Still further increases in pressure drop do not change c_g and the membrane is said to be "gel polarized." Then Eq. (13.11-3) becomes (P1, P6, R1)

Equation 13.11-5.

$$\frac{N_w}{\rho} = k_c \ln\left(\frac{c_g}{c_1}\right)$$

With increases in pressure drop, the gel layer increases in thickness, causing the solvent flux to decrease because of the added gel-layer resistance. Finally, the net flux of solute by convective transfer becomes equal to the back diffusion of solute into the bulk solution because of the polarized concentration gradient, as given by Eq. (13.11-5).

The added gel-layer resistance next to the membrane causes an increased resistance to solvent flux, as given by

Equation 13.11-6.

$$N_w = \frac{\Delta P}{1/A_w + R_g}$$

where $1/A_w$ is the membrane resistance and R_g is the variable gel-layer resistance, (s · m^2 · atm)/kg solvent. The solvent flux in this gel-polarized regime is independent of pressure difference and is determined by Eq. (13.11-5) for back diffusion. Experimental data confirm the use of Eq. (13.11-5) for a large number of macromolecular solutions, such as proteins and so forth as well as colloidal suspensions, such as latex particles and so forth (P1, P6).

Effects of Processing Variables in Ultrafiltration

A plot of typical experimental data for flux versus pressure difference is shown in Fig. 13.11-2 (H1, P6). At low pressure differences and/or low solute concentrations, the data typically follow Eq. (13.11-1). For a given bulk concentration, c_1, the flux approaches a constant value at high pressure differences, as shown in Eq. (13.11-5). Also, more-dilute protein concentrations give higher flux rates, as expected from Eq. (13.11-5). Most commercial applications are flux-limited by concentration polarization and operate in the region where the flux is approximately independent of pressure difference (R1).

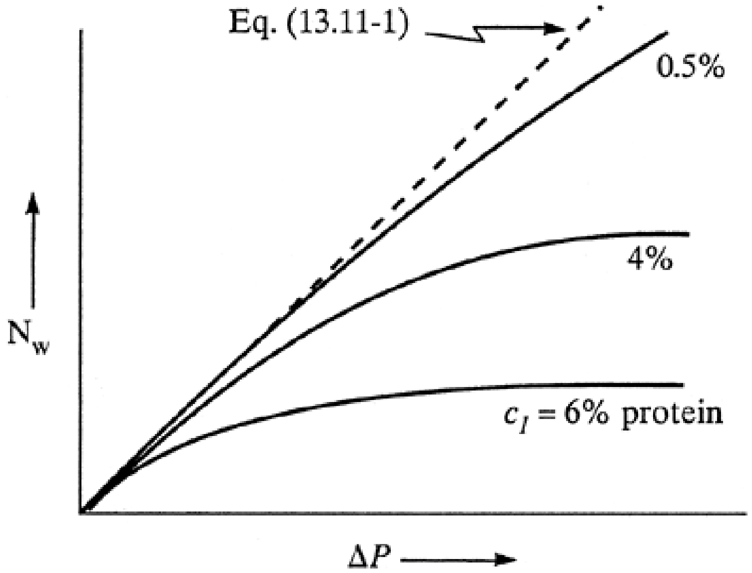

Figure 13.11-2. Effect of pressure difference on solvent flux.

Using experimental data, a plot of N_w/p versus ln c_1 is a straight line with a negative slope of k_c, the mass-transfer coefficient, as shown by Eq. (13.11-5). These plots also give the value of c_g, the gel concentration. Data (*P1*) show that the gel concentration for many macromolecular solutions is about 25 wt %, with a range of 5 to 50%. For colloidal dispersions it is about 65 wt %, with a range of 50 to 75%.

The concentration-polarization effects for hollow fibers are often quite small, due to the low solvent flux. Hence, Eq. (13.11-1) describes the flux. In order to increase the ultrafiltration solvent flux, cross-flow of fluid past the membrane can be used to sweep away part of the polarized layer, thereby increasing k_c in Eq. (13.11-5). Higher velocities and other methods are used to increase turbulence and hence k_c. In most cases the solvent flux is too small to operate in a single-pass mode. It is necessary to recirculate the feed past the membrane, with recirculation rates of 10/1 to 100/1 often used.

Methods for predicting the mass-transfer coefficient k_c in Eq. (13.11-5) are given by others (P1, P6) for known geometries such as channels and so forth. Predictions of flux in known geometries using these methods and experimental values of c_g in Eq. (13.11-5) in the gel polarization regime compare with experimental values for macromolecular solutions within about 25–30%. However, for colloidal dispersions the experimental flux is higher than the theoretical by factors of 20-30 for laminar flow and 8-10 for turbulent flow. Hence, Eq. (13.11-5) is not useful for predicting the solvent flux accurately. Generally, for design of commercial units it is necessary to obtain experimental data on single modules.

MICROFILTRATION MEMBRANE PROCESSES

Introduction

In microfiltration, pressure-driven flow through a membrane is used to separate micron-size particles from fluids. The size range of particles ranges from 0.02 μm to 10 μm (H2). This microfiltration separates particles from solutions. The particles are usually larger than the solutes in reverse osmosis and ultrafiltration. Hence, osmotic pressure is negligible. At the very low end of the size range, very large soluble macromolecules are retained. Bacteria and other microorganisms (P7) are also retained on these membranes. Other particles in this size range are paint pigment, yeast cells, suspended matter such as cells from fermentation broth, particles in beer pasteurization, and so on. The dividing line between ultrafiltration and microfiltration is not very distinct.

The pore sizes of the membranes and the permeate flux are typically larger than for reverse osmosis and ultrafiltration. Usually the pressure drop used across the membranes varies from 1 psi to 50 psi (H2). Types of membranes are extremely varied and can be ceramics, polymers, and so on.

Many different geometries of membranes are used. These include spiral-wound, plate and frame, hollow fiber, cartridge filters with pleated membranes, and so on. Disposable cartridges are also used.

Models for Microfiltration

Dead-end microfiltration flow model

In many laboratory batch filtrations, the batch process is run in dead-end flow, with the membrane replacing the conventional filter paper. The particles build up with time as a cake and the clarified permeate is forced through the membrane, as shown in Fig. 13.12-1a. The permeate flux equation is (H2)

Equation 13.12-1.

$$N_w = \frac{\Delta P}{\mu(R_m + R_c)}$$

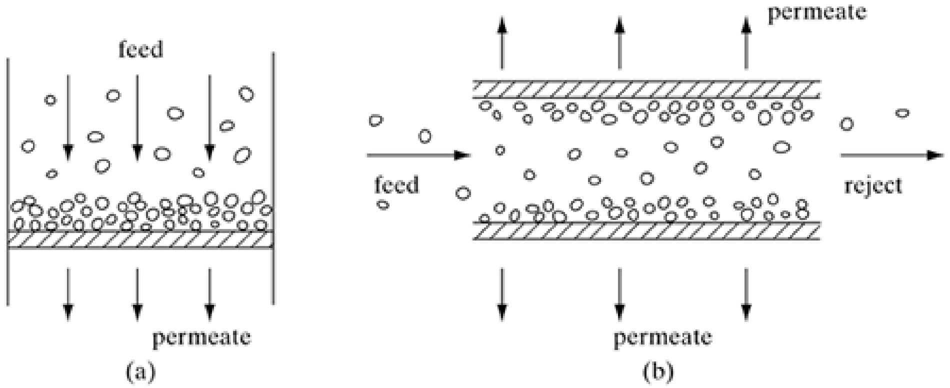

Figure 13.12-1. Process flow for microfiltration: (a) dead-end flow, (b) cross-flow.

where N_w is the solvent flux in kg/(s · m^2), ΔP is the pressure difference in Pa, μ is viscosity of the solvent in Pa · s, R_m is the membrane resistance in m^2/kg, and R_c is the cake resistance in m^2/kg, which increases with time due to cake buildup.

This Eq. (13.12-1) is similar to Eq. (14.2-8) for ordinary filtration given in Section 14.2 of this text. Solutions to this equation are also given there.

Cross-flow microfiltration flow model

In the cross-flow model shown in Fig. 13.12-1b, the operation is similar to that for reverse osmosis and ultrafiltration in that the flow of bulk solution is parallel to the membrane surface and not through it (H2). The permeate flow through the membrane carries particles to the surface, where they form a thin layer. A relatively high flow rate tangential to the surface sweeps the deposited particles toward the filter exit leaving a relatively thin deposited cake layer. This thin cake layer is similar to the gel layer formed in ultrafiltration. This cross-flow is effective in controlling concentration polarization and cake buildup, allowing relatively high fluxes to be maintained.

This concentration-polarization model of convection of particles to the cake layer is balanced by particle diffusion by Brownian diffusion away from the cake surface. This model is similar to the flux Eq. (13.11-3) for ultrafiltration. Other models are also given elsewhere (H2).

PROBLEMS

13.2-1. ***Diffusion Through Liquids and a Membrane.*** A membrane process is being designed to recover solute A from a dilute solution where $c_1 = 2.0 \times 10^{-2}$ kg mol A/m^3 by dialysis through a membrane to a solution where $c_2 = 0.3 \times 10^{-2}$. The membrane thickness is 1.59×10^{-5} m, the distribution coefficient $K' = 0.75$, $D_{AB} = 3.5 \times 10^{-11}$ m^2/s in the membrane, the mass-transfer coefficient in the dilute solution is $k_{c1} = 3.5 \times 10^{-5}$ m/s, and $k_{c2} = 2.1 \times 10^{-5}$.

a. Calculate the individual resistances, total resistance, and total percent resistance of the two films.

b. Calculate the flux at steady state and the total area in m^2 for a transfer of 0.01 kg mol solute/h.

c. Increasing the velocity of both liquid phases flowing past the surface of the membrane will increase the mass-transfer coefficients, which are approximately proportional to $v^{0.6}$, where v is velocity. If the velocities are doubled, calculate the total percent resistance of the two films and the percent increase in flux.

A1: **Ans.** (a) Total resistance = 6.823×10^5 s/m, 11.17% resistance; (b) $N_A = 2.492 \times 10^{-8}$ kg mol A/s · m^2, area = 111.5 m^2

13.2-2. ***Suitability of a Membrane for Hemodialysis.*** Experiments are being conducted to determine the suitability of a cellophane membrane 0.029 mm thick for use in an artificial-kidney device. In an experiment at 37°C using NaCl as the diffusing solute, the membrane separates two components containing stirred aqueous solutions of NaCl, where $c_1 = 1.0 \times 10^{-4}$ g mol/cm^3 (100 g mol/m^3) and $c_2 = 5.0 \times 10^{-7}$. The mass-transfer coefficients on either side of the membrane have been estimated as $k_{c1} = k_{c2} = 5.24 \times 10^{-5}$ m/s. Experimental data obtained gave a flux $N_A = 8.11 \times 10^{-4}$ g mol NaCl/s · m^2 at pseudo-steady-state conditions.

a. Calculate the permeability p_M in m/s and $D_{AB}K'$ in m^2/s.

b. Calculate the percent resistance to diffusion in the liquid films.

13.3-1. ***Gas-Permeation Membrane for Oxygenation.*** To determine the suitability of silicone rubber for its use as a membrane for a heart-lung machine to oxygenate blood, an experimental value of the permeability at 30°C of oxygen was obtained, where $P_M = 6.50 \times 10^{-7}$ cm^3 O$_2$ (STP)/(s · cm^2 · cm Hg/mm).

a. Predict the maximum flux of O$_2$ in kg mol/s · m^2 with an O$_2$ pressure of 700 mm Hg on one side of the membrane and an equivalent pressure in the blood film side of 50 mm. The membrane is 0.165 mm thick. Since the gas film is pure oxygen, the gas film resistance is zero. Neglect the blood film resistance in this case.

b. Assuming a maximum requirement for an adult of 300 cm^3 O$_2$ (STP) per minute, calculate the membrane surface area required in m^2. (*Note:* The actual area needed should be considerably larger since the blood film resistance, which must be determined by experiment, can be appreciable.)

A3: **Ans.** (b) 1.953 m^2

13.4-1. ***Derivation of Equation for Permeate Concentration.*** Derive Eq. (13.4-11) for Case 2 for complete mixing. Note that x_o from Eq. (13.4-9) must first be substituted into Eq. (13.4-6) before multiplying out the equation and solving for y_p.

13.4-2. ***Use of Complete-Mixing Model for Membrane Design***. A membrane having a thickness of 2×10^{-3} cm, permeability $P'_A = 400 \times 10^{-10}$ cm^3 (STP) · cm/(s · cm^2 · cm Hg), and $\alpha^* = 10$ is to be used to separate a gas mixture of A and B. The feed flow rate is $L_f = 2 \times 10^3$ cm^3 (STP)/s and its composition is $x_f = 0.413$. The feed-side pressure is 80 cm Hg and the permeate-side pressure is 20 cm Hg. The reject composition is to be $x_o = 0.30$. Using the complete-mixing model, calculate the permeate composition, fraction of feed permeated, and membrane area.

A5: **Ans.** $y_p = 0.678$

13.4-3. ***Design Using Complete-Mixing Model.*** A gaseous feed stream having a composition $x_f = 0.50$ and a flow rate of 2×10^3 cm^3 (STP)/s is to be separated in a membrane unit. The feed-side pressure is 40 cm Hg and the permeate is 10 cm Hg. The membrane has a thickness of 1.5×10^{-3} cm, permeability $P'_A = 40 \times 10^{-10}$ cm^3 (STP) cm/(s · cm^2 · cm Hg), and $\alpha^* = 10$. The fraction of feed permeated is 0.529.

a. Use the complete-mixing model to calculate the permeate composition, reject composition, and membrane area.

b. Calculate the minimum reject concentration.

c. If the feed composition is increased to $x_f = 0.60$, what is this new minimum reject concentration?

A6: **Ans.** (a) $A_m = 5.153 \times 10^7$ cm^2 (c) $x_{oM} = 0.2478$

13.4-4. ***Effect of Permeabilities on Minimum Reject Concentration.*** For the conditions of Problem 13.4-2, $x_f = 0.413$, $\alpha^* = 10$, $p_l = 20$ cm Hg, $p_h = 80$ cm Hg, and $x_o = 0.30$. Calculate the minimum reject concentration for the following cases:

a. Calculate x_{oM} for the given conditions.

b. Calculate the effect on x_{oM} if the permeability of B increases so that α^* decreases to 5.

c. Calculate the limiting value of x_{oM} when α^* is lowered to its minimum value of 1.0. Make a plot of x_{oM} versus α^* for these three cases.

13.4-5. ***Minimum Reject Concentration and Pressure Effect.*** For Example 13.4-2 for separation of air, do as follows:

a. Calculate the minimum reject concentration.

b. If the pressure on the feed side is reduced by one-half, calculate the effect on x_{oM}.

A8: **Ans.** (b) $x_{oM} = 0.0624$

13.5-1. ***Separation of Multicomponent Gas Mixtures.*** Using the same feed composition and flow rate, pressures, and membrane as in Example 13.5-1, do the following, using the complete-mixing model:

a. Calculate the permeate composition, reject composition, and membrane area for a fraction permeated of 0.50 instead of 0.25.

b. Repeat part (a) but for $\theta = 0.90$.

c. Make a plot of permeate composition y_{pA} versus θ and also of area A_m versus θ using the calculated values for $\theta = 0.25$, 0.50, and 0.90.

13.5-2. ***Separation of Helium from Natural Gas.*** A typical composition of a natural gas (S1) is 0.5% He (A), 17.0% N_2 (B), 76.5% CH_4 (C), and 6.0% higher hydrocarbons (D). The membrane proposed to separate helium has a thickness of 2.54×10^{-3} cm, and the permeabilities are $P'_A = 60 \times 10^{-10}$ cm^3 (STP) · cm/(s · cm^2 · cm Hg), $P'_B = 3.0 \times 10^{-10}$, and $P'_C = 1.5 \times 10^{-10}$. It is assumed that the higher hydrocarbons are essentially nonpermeable ($P'_D \cong 0$). The feed flow rate is 2.0×10^5 cm^3 (STP)/s. The feed pressure $p_h = 500$ cm Hg and the permeate pressure $p_l = 20$ cm Hg.

a. For a fraction permeated of 0.2, calculate the permeate composition, reject composition, and membrane area using the complete mixing model.

b. Use the permeate from part (a) as feed to a completely mixed second stage. The pressure $p_h = 500$ cm Hg and $p_l = 20$ cm. For a fraction permeated of 0.20, calculate the permeate composition and membrane area.

13.6-1. ***Design Using Cross-Flow Model for Membrane.*** Use the same conditions for the separation of an air stream as given in Example 13.6-1. The given values are $x_f = 0.209$, $\alpha^* = 10$, $p_h = 190$ cm Hg, $p_l = 19$ cm Hg, $L_f = 1 \times 10^6$ cm^3 (STP)/s, $P'_A = 500 \times 10^{-10}$ cm^3 (STP) · cm/(s · cm^2 · cm Hg), and $t = 2.54 \times 10^{-3}$ cm. Do as follows using the cross-flow model:

a. Calculate y_p, x_o, and A_m for $\theta = 0.40$.

b. Calculate y_p and x_o for $\theta = 0$.

A11: **Ans.** (a) $y_p = 0.452$, $x_o = 0.0303$, $A_m = 6.94 \times 10^8$ cm^2 (S6); (b) $y_p = 0.655$, $x_o = 0.209$

13.7-1. ***Equations for Cocurrent and Countercurrent Flow Models.*** Derive the equations for the following cases:

a. For cocurrent flow, show the detailed steps for deriving Eqs. (13.7-35) and (13.7-36).

b. For countercurrent flow, show the detailed steps in obtaining Eq. (13.7-22) from (13.7-4) and (13.7-5). Also, show the detailed steps to derive Eq. (13.7-24).

13.7-2. ***Design Using Countercurrent-Flow Model for Membrane.*** Use the same conditions as given in Example 13.6-1 for the separation of an air stream. The given values are $x_f = 0.209$, $\alpha^* = 10$, $p_h = 190$ cm Hg, $p_l = 19$ cm Hg, $L_f = 1 \times 10^6$ cm^3 (STP)/s, $P'_A = 500 \times 10^{-10}$ cm^3 (STP) · cm/(s · cm^2 · cm Hg), and $t = 2.54 \times 10^{-3}$ cm. Using the countercurrent-flow model, calculate y_p, x_o, and A_m for $\theta = 0.40$. (Note that this problem involves a trial-and-error procedure along with the numerical solution of two differential equations.)

13.8-1. ***Effect of Pressure Drop on Asymmetric Membrane Calculations.*** Using the same conditions as in Example 13.8-1, do as follows:

a. Use the shortcut method to calculate the overall pressure drop Δp_h using Eq. (13.8-16) over the entire length. Use typical data for air given in Section 13.8C to calculate N_T, fiber length $z_2 - z_1$, and so forth. Assume $T = 25° + 273$ K and $p_h = 1034$ kPa, $T_s = 273$ K, $p_s = 101.325$ kPa.

b. With the above values of p_h, use the shortcut method in a second iteration to recalculate A_m. (Be sure to correct for P_{ho} at x_o and y'_o).

c. Calculate the pressure drop if the number of tubes N_T in part (a) is reduced by 50%.

A14: **Ans.** (a) $N_T = 1.267 \times 10^5$, $(z_2 - z_1) = 1.413$ m, $\Delta p_h = 20.74$ kPa; (b) $A_m = 54.10$ m^2; (c) $\Delta p_h = 82.96$ kPa

13.8-2. ***Spreadsheet Calculation for Asymmetric Membrane.*** Using the conditions for Example 13.8-1, write the detailed spreadsheet and calculate the results. Compare these results with those in Table 13.8-2.

13.8-3. ***Comparison of Experimental and Predicted Spreadsheet Results in a Pilot-Unit Asymmetric Membrane.*** A pilot-size membrane used to separate air in order to obtain nitrogen has the following dimensions with the feed inside the tubes: total $N_T = 3.8 \times 10^4$ fibers, ID = 95 μm, OD = 135 μm, length of fibers = 19 in. An experimental run gave the following results. Feed rate $L_f = 1.086$ m^3/h, $L_o = 0.654$ m^3/h, $V_p = 0.450$ m^3/h, $x_o = 0.067$ mole fraction oxygen, $y_p = 0.413$, $p_h = 703.81$ kPa, $p_l = 98.10$ kPa, and $T = 25$°C. The permeances determined previously are $(P'_{O_2}/t) = 1.50 \times 10^{-10}$ m^3 (STP)/(s · m^2 · Pa), $(P'_{N_2}/t) = 2.47 \times 10^{-11}$. Flow is counter current. Do as follows:

a. Predict the pressure drop in the tubes using the shortcut method.

b. Using a spreadsheet, predict the performance of this run and compare these results with the experimental values. Note that this is trial and error, since the area is fixed but the value of x_o is not. First assume a value of x_o. Then divide the difference between $x_f = 0.209$ and x_o into nine equal parts and perform the spreadsheet calculation. If the calculated and actual areas do not agree, assume another value of x_o, and so forth. Neglect pressure drop.

A16: **Ans.** (a) $\Delta p_h = 4.455$ kPa; (b) $x_o = 0.079$, $V_p = 0.442$ m^3/hr, $y_p = 0.398$

13.9-1. ***Osmotic Pressure of Salt and Sugar Solutions.*** Calculate the osmotic pressure of the following solutions at 25°C and compare with the experimental values:

a. Solution of 0.50 g mol NaCl/kg H_2O. (See Table 13.9-1 for the experimental value.)

b. Solution of 1.0 g sucrose/kg H_2O. (Experimental value = 0.0714 atm.)

c. Solution of 1.0 g $MgCl_2$/kg H_2O. (Experimental value = 0.660 atm.)

A17: **Ans.** (a) $\pi = 24.39$ atm; (b) $\pi = 0.0713$ atm; (c) $\pi = 0.768$ atm

13.9-2. ***Determination of Permeability Constants for Reverse Osmosis.*** A cellulose-acetate membrane with an area of 4.0×10^{-3} m^2 is used at 25°C to determine the permeability constants for reverse osmosis of a feed salt solution containing 12.0 kg NaCl/m^3 (ρ = 1005.5 kg/m^3). The product solution has a concentration of 0.468 kg NaCl/m^3 (ρ = 997.3 kg/m^3). The measured product flow rate is 3.84×10^{-8} m^3/s and the pressure difference used is 56.0 atm. Calculate the permeability constants and the solute rejection R.

A18: **Ans.** $A_w = 2.013 \times 10^{-4}$ kg solvent/s · m^2 · atm, $R = 0.961$

13.9-3. ***Performance of a Laboratory Reverse-Osmosis Unit.*** A feed solution at 25°C contains 3500 mg NaCl/L (ρ = 999.5 kg/m^3). The permeability constant $A_w = 3.50 \times 10^{-4}$ kg solvent/s · m^2 · atm and $A_s = 2.50 \times 10^{-7}$ m/s. Using a ΔP = 35.50 atm, calculate the fluxes, solute rejection R, and product solution concentration in mg NaCl/L. Repeat, but using a feed solution of 3500 mg BaCl$_2$/L. Use the same value of A_w, but $A_s = 1.00 \times 10^{-7}$ m/s (A1).

13.10-1. ***Effect of Pressure on Performance of Reverse-Osmosis Unit.*** Using the same conditions and permeability constants as in Example 13.10-1, calculate the fluxes, solute rejection R, and product concentration c_2 for ΔP pressures of 17.20, 27.20, and 37.20 atm. *(Note:* The values for 27.20 atm have already been calculated.) Plot the fluxes, R, and c_2 versus the pressure.

13.10-2. ***Effect of Concentration Polarization on Reverse Osmosis.*** Repeat Example 13.10-1 but use a concentration polarization of 1.5. *(Note:* The flux equations and the solute rejection R should be calculated using this new value of c_1.)

A21: **Ans.** $N_w = 1.171 \times 10^{-2}$ kg solvent/s · m^2, c_2 = 0.1361 kg NaCl/m^3

13.10-3. ***Performance of a Complete-Mixing Model for Reverse Osmosis.*** Use the same feed conditions and pressures given in Example 13.10-1. Assume that the cut or fraction recovered of the solvent water will be 0.10 instead of the very low water recovery assumed in Example 13.10-1. Hence, the concentrations of the entering feed solution and the exit feed will not be the same. The flow rate q_2 of the permeate water solution is 100 gal/h. Calculate c_1 and c_2 in kg NaCl/m^3 and the membrane area in m^2.

A22: **Ans.** c_1 = 2.767 kg/m^3, c_2 = 0.0973 kg/m^3, area = 8.68 m^2

13.11-1. ***Flux for Ultrafiltration.*** A solution containing 0.9 wt % protein is to undergo ultrafiltration using a pressure difference of 5 psi. The membrane permeability is $A_w = 1.37 \times 10^{-2}$ kg/s · m^2 · atm. Assuming no effects of polarization, predict the flux in kg/s · m^2 and in units of gal/ft^2 · day, which are often used in industry.

A23: **Ans.** 9.88 gal/ft^2 · day

13.11-2. ***Time for Ultrafiltration Using Recirculation.*** It is desired to use ultrafiltration for 800 kg of a solution containing 0.05 wt % of a protein to obtain a solution of 1.10 wt %. The feed is recirculated past the membrane with a surface area of 9.90 m^2. The permeability of the membrane is $A_w = 2.50 \times 10^{-2}$ kg/s · m^2 · atm. Neglecting the effects of concentration polarization, if any, calculate the final amount of solution and the time to achieve this, using a pressure difference of 0.50 atm.

REFERENCES

Bibliography

[ch13biblio01entry01] (Al) J. P., Agrawal, and S. Sourirajan, *Ind. Eng. Chem.*, **69**(11), 62 (1969).

[ch13biblio01entry02] (B1) C. T., Blaisdell, and K. Kammermeyer, *Chem. Eng. Sci.*, **28**, 1249 (1973).

[ch13biblio01entry03] (B2) A. L., Babb, C. J., Maurer, D. L., Fry, R. P, Popovich, and R. E. McKee, *Chem. Eng. Progr. Symp.*, **64**(84), 59 (1968).

[ch13biblio01entry04] (B3) R. I. Berry, *Chem. Eng.*, **88** (July 13), 63 (1981).

[ch13biblio01entry05] (C1) W. E. Clark, *Science*, **138**, 148 (1962).

[ch13biblio01entry06] (G1) S., Giglia, B., Bikson, and J. E. Perrin, *Ind. Eng. Chem. Res.*, **30**, 1239 (1991).

[ch13biblio01entry07] (H1) S. T., Hwang, and K. Kammermeyer, *Membranes in Separations*. New York: John Wiley & Sons, Inc., 1975.

[ch13biblio01entry08] (H2) W. S., Ho, and K. K. Sirkar, *Membrane Handbook*. New York: Van Nostrand Reinhold, 1992.

[ch13biblio01entry09] (K1) S., Kimura, and S. Sourirajan, *A.I.Ch.E. J.*, **13**, 497 (1967).

[ch13biblio01entry10] (K2) E. C. Kaup, *Chem. Eng.*, **80** (Apr. 2), 46 (1973).

[ch13biblio01entry11] (L1) R. E. Lacey, *Chem. Eng.*, **79** (Sept. 4), 57 (1972).

[ch13biblio01entry12] (M1) W. L. McCabe, *Ind. Eng. Chem.*, **21**, 112 (1929).

[ch13biblio01entry13] (M2) A. S. Michaels, *Chem. Eng. Progr.*, **64**(12), 31 (1968).

[ch13biblio01entry14] (M3) Merten,U. (ed.). *Desalination by Reverse Osmosis*. Cambridge, Mass.: The MIT Press, 1966.

[ch13biblio01entry15] (M4) S. L., Matson, J., Lobez, and J. A. Quinn, *Chem. Eng. Sci.*, **38**, 503 (1983).

[ch13biblio01entry16] (M5) W. L., Mccabe, J. C., Smith, and P. Harriott, *Unit Operations of Chemical Engineering*, 5th ed. New York: McGraw-Hill Book Company, 1993.

[ch13biblio01entry17] (N1) R. D., Noble, and S. A. Stern, *Membrane Separations Technology: Principles and Applications*. Amsterdam: Elsevier Science, 1995.

[ch13biblio01entry18] (P1) R. H., Perry, and D. Green, *Perry's Chemical Engineers' Handbook*, 6th ed. New York: McGraw-Hill Book Company, 1984.

[ch13biblio01entry19] (P2) C. Y. Pan, *A.I.Ch.E. J.*, **29**, 545 (1983).

[ch13biblio01entry20] (P3) Permasep Permeators. *E. I. duPont Tech. Bull.*, 401, 403, 405 (1972).

[ch13biblio01entry21] (P4) C. Y., Pan, and H. W. HABGOOD, *Ind. Eng. Chem. Fund.*, **13**, 323 (1974).

[ch13biblio01entry22] (P5) C. Y., Pan, and H. W. Habgood, *Can. J. Chem. Eng.*, **56**, 197, 210 (1978).

[ch13biblio01entry23] (P6) Porter,M.C. (ed.). *Handbook of Industrial Membrane Technology*. Park Ridge, N.J.: Noyes Publications, 1990.

[ch13biblio01entry24] (P7) R. H., Perry, and D. Green, *Perry's Chemical Engineers' Handbook*, 7th ed. New York: McGraw-Hill Book Company, 1997.

[ch13biblio01entry25] (R1) Rousseau,R.W. (ed.). *Handbook of Separation Process Technology*. New York: John Wiley & Sons, Inc., 1987.

[ch13biblio01entry26] (S1) S. A., Stern, T. F., Sinclair, P. J., Gareis, N. P., Vahldieck, and P. H. Mohr, *Ind. Eng. Chem.*, **57**, 49 (1965).

[ch13biblio01entry27] (S2) V. T., Stannett, W. J., Koros, D. R., Paul, H. K., Lonsdale, and R. W. Baker, *Adv. Polym. Sci.*, **32**, 69 (1979).

[ch13biblio01entry28] (S3) R. W., Stoughten, and M. H., Lietzke,, Jr. *Chem. Eng. Data*, **10**, 254 (1965).

[ch13biblio01entry29] (S4) E. D. Schroeder, *Water and Wastewater Treatment*. New York: McGraw-Hill Book Company, 1977.

[ch13biblio01entry30] (S5) S. Sourirajan, *Reverse Osmosis*. New York: Academic Press, Inc., 1970.

[ch13biblio01entry31] (S6) S. A., Stern, and W. P. Walawender, *Sep. Sci.*, **4**, 129 (1969).

[ch13biblio01entry32] (S7) D. J., Stookey, C. J., Patton, and G. L. Malcolm, *Chem. Eng. Progr.*, **82**(11), 36 (1986).

[ch13biblio01entry33] (W1) W. J., Weber,, Jr. *Physicochemical Processes for Water Quality Control*. New York: Wiley-Interscience, 1972.

[ch13biblio01entry34] (W2) W. J., Ward, W. R., Browal, and R.M. J. Salemme, *Membr. Sci.*, **1**, 99 (1976).

[ch13biblio01entry35] (W3) S., Weller, and W. A. Steiner, *Chem. Eng. Progr.*, **46**, 585 (1950).

[ch13biblio01entry36] (W4) S., Weller, and W. A. Steiner, *J. Appl. Phys.*, **21**, 279 (1950).

[ch13biblio01entry37] (W5) W. P., Walawender, and S. A. Stern, *Sep. Sci.*, **7**, 553 (1972).